# Semiconductor Detectors
# applications in basic science and industry

OUTLINE Part II:

1. Semiconductors based on sideward depletion

   (a) the SDD with integrated FET

   (b) the pnCCD

   (c) the CDD

   (d) the DEPFET (active pixel sensor)

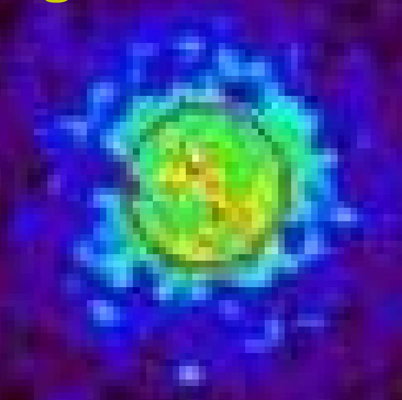

2. Avalanche amplifiers
3. Summary and Conclusion

# Semiconductors as detector and electronics material

1. **Semiconductors: $E_{Gap} \approx 1 - 3$ eV**
   **→ small leakage currents**
   **→ low noise, operation @ r.t.**

2. **Pair creation energy: w = 2 – 5 eV**
   **→ large number of signal charges per energy deposit in detector**

3. **Density: $\rho = 2 - 10\ g\ cm^{-3}$**
   **→ high energy loss per unit length**
   **→ low range of δ - electrons**

***This leads to:***

good energy resolution
high spatial resolution
high quantum and detection efficieny
good mechanical regidity and thermal conductivity

***Semiconductors equally offer:***

fixed space charges
high mobility of charge carriers

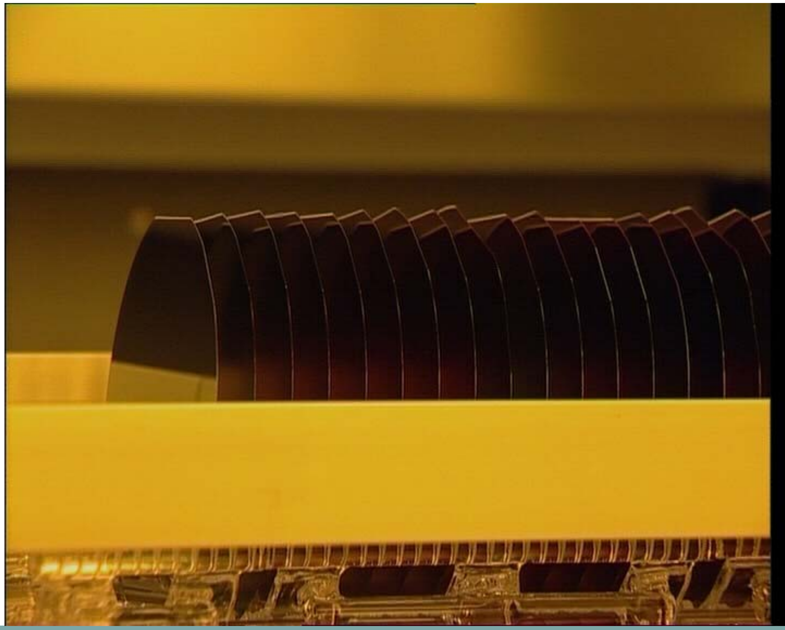

# Problem with planar diodes

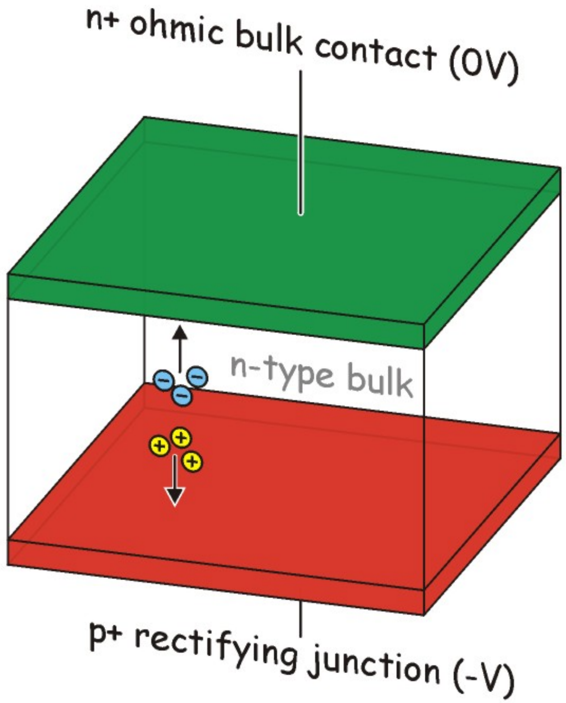


electronic noise

$$ENC = \sqrt{\underbrace{a \frac{2kT}{g_m} C_{tot}^2 A_1 \frac{1}{\tau}}_{\text{thermal noise}} + \underbrace{2\pi a_f C_{tot}^2 A_2}_{\text{1/f noise}} + \underbrace{q I_L A_3 \tau}_{\text{leakage}}}$$

optimum shaping time

$$\tau_{opt} = \sqrt{\frac{2A_3}{A_1} \frac{kT}{q} \frac{C_{tot}^2}{I_L} \frac{2}{3g_m}}$$

» For

- **good resolution**
- **high count rate capability**

the total capacitance must be minimised!!

# Limits of energy resolution

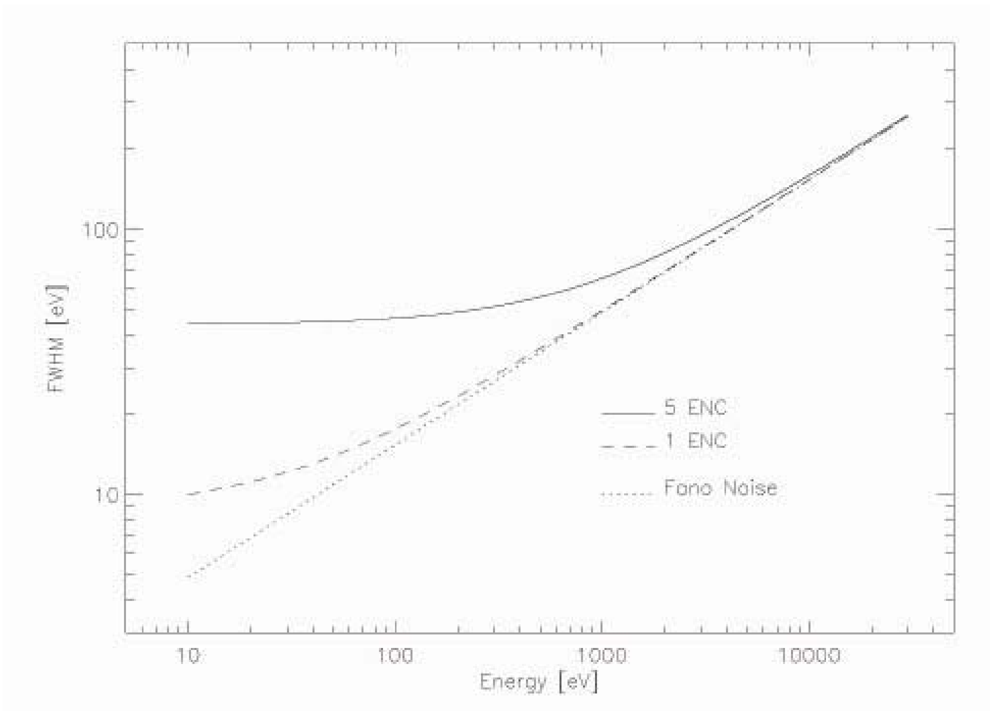


$$ENC^2_{fano} = \frac{F \cdot E}{w}$$

$$ENC^2_{trans} \approx (1 - CTE)\, N_{trans}$$

$$ENC^2 = \left(\alpha \frac{2kT}{g_m} C^2{}_{tot} A_1\right)\frac{1}{\tau} + \left[\left(2\pi a_f C^2{}_{tot} + \frac{b_f}{2\pi}\right) A_2\right] + \left(q I_l + \frac{2kT}{R_f} A_3\right)\tau$$

$$ENC^2_{tot} = ENC^2_{el} + ENC^2_{fano} + ENC^2_{trans} + \ldots$$

# Noise analysis

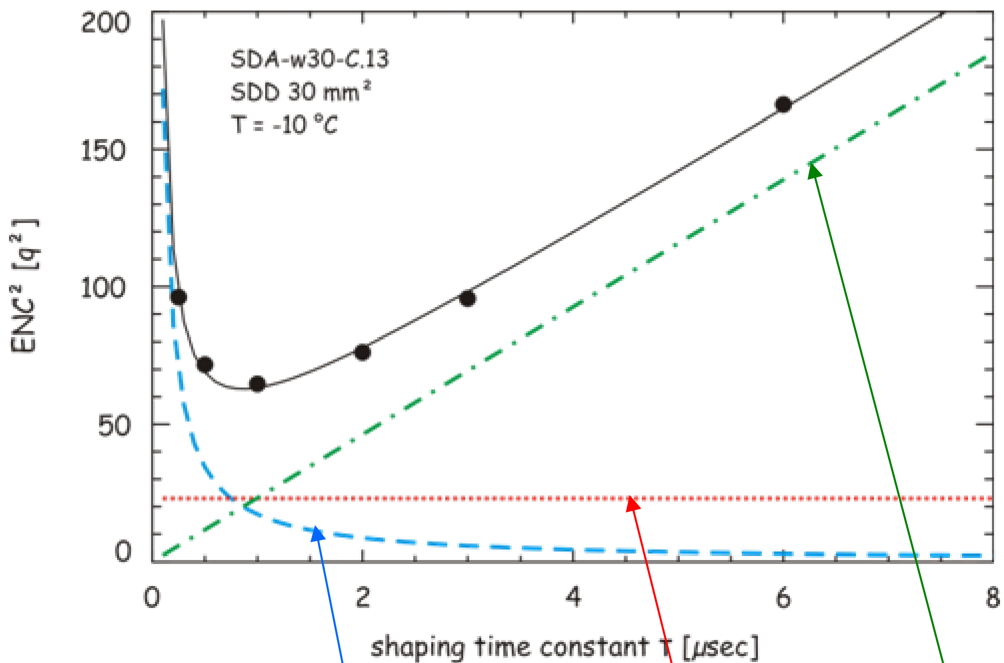


$$ENC^2 = a\frac{2kT}{g_m}C_{tot}^2 A_1 \frac{1}{\tau} + 2\pi a_f C_{tot}^2 A_2 + qI_L A_3 \tau$$

thermal noise | 1/f noise | leakage current

multi-parameter fit

» extraction of
- total capacitance $C_{tot}$
- 1/f noise coeff. $a_f$
- leakage current $I_L$

independent measurement of
- transconductance $g_m$ (180 … 250 μS)

$A_i$ = filter constants (Gaussian 6th order)

τ = shaping time constant

q = electron charge

a = 2/3 for FET in saturation

# Sideward Depletion Structure

Emilio Gatti & Pavel Rehak, 1984

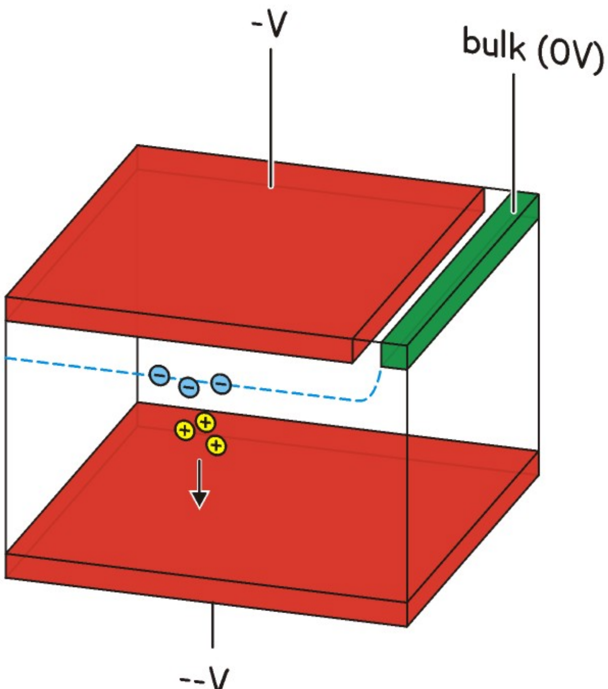


asymmetric bias

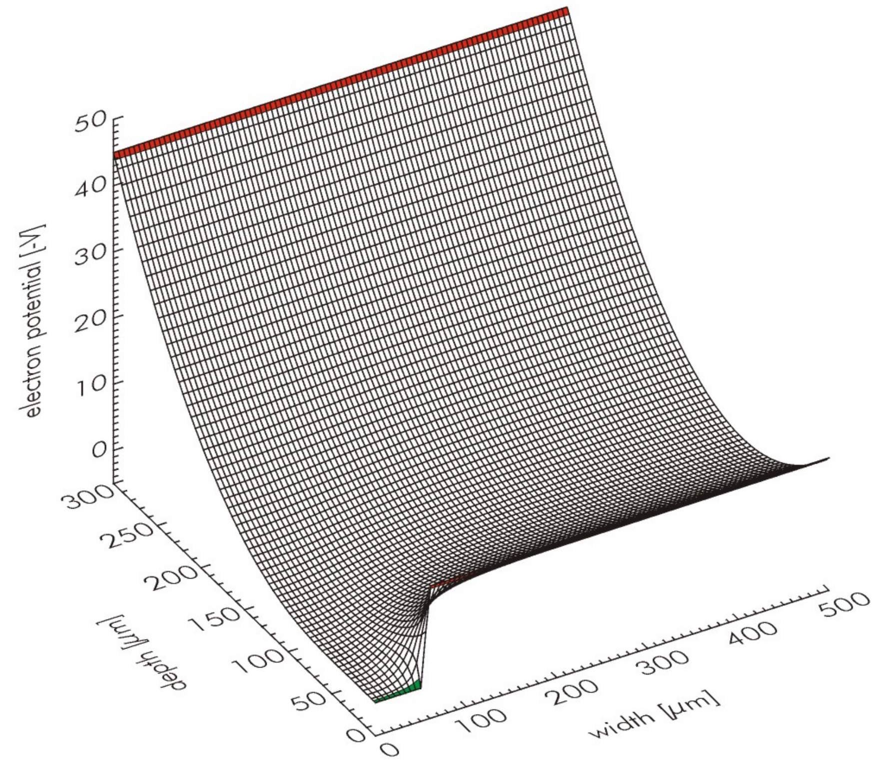


- fully depleted volume
- minimum capacitance of bulk contact (independent of sensitive area)

**?? signal extraction ??**

» advanced detector concepts

# Silicon Drift Detector (SDD)

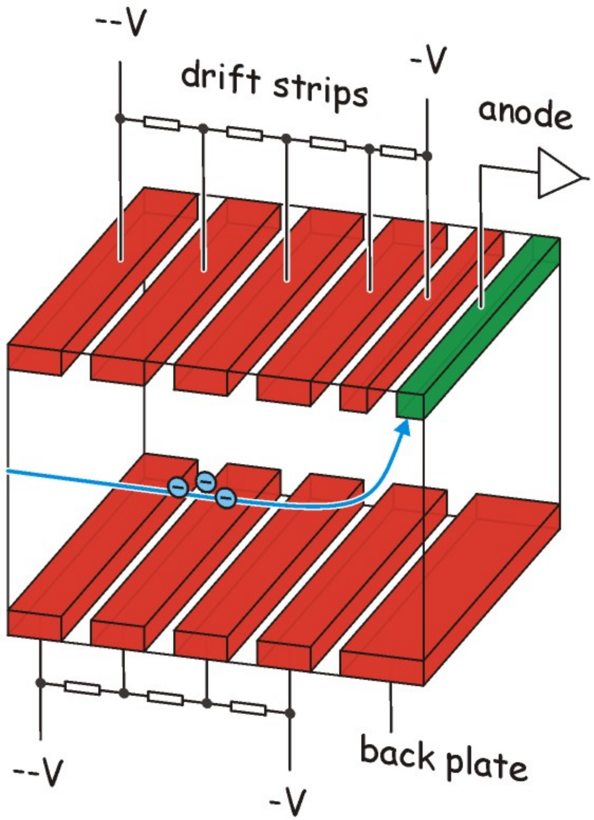


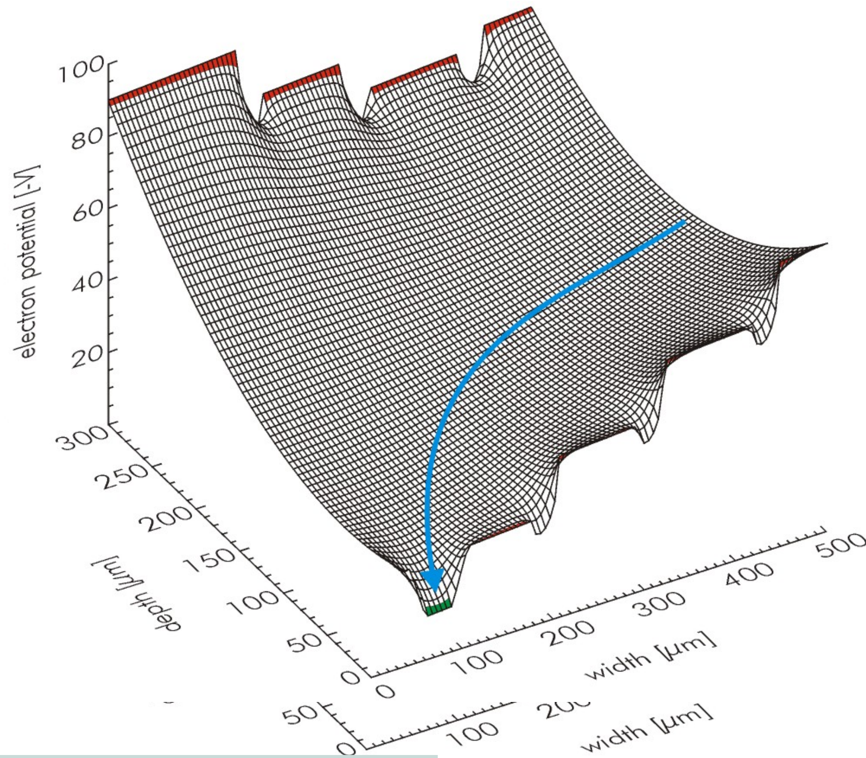


- drift field || surface
- 1D position resolution by drift time measurement start trigger!!

# Silicon Drift Detector (SDD)

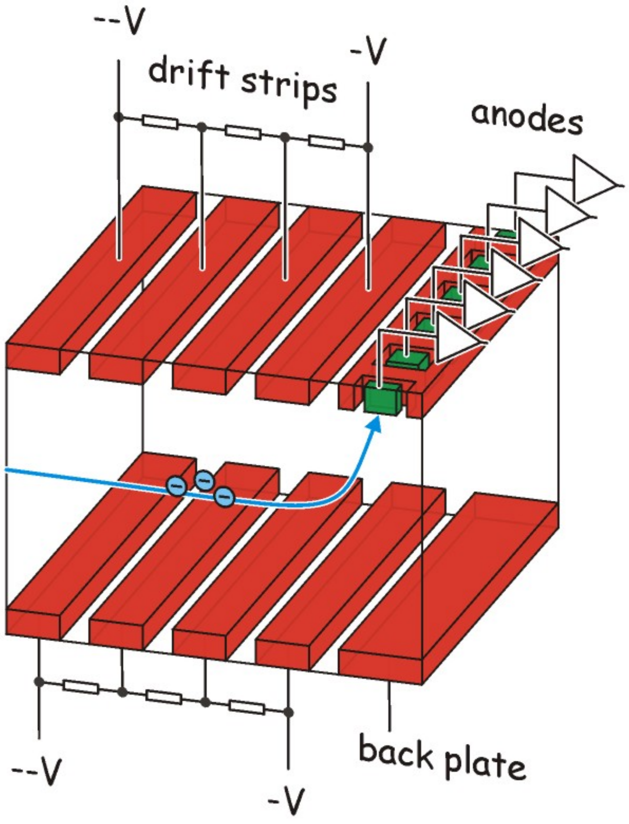


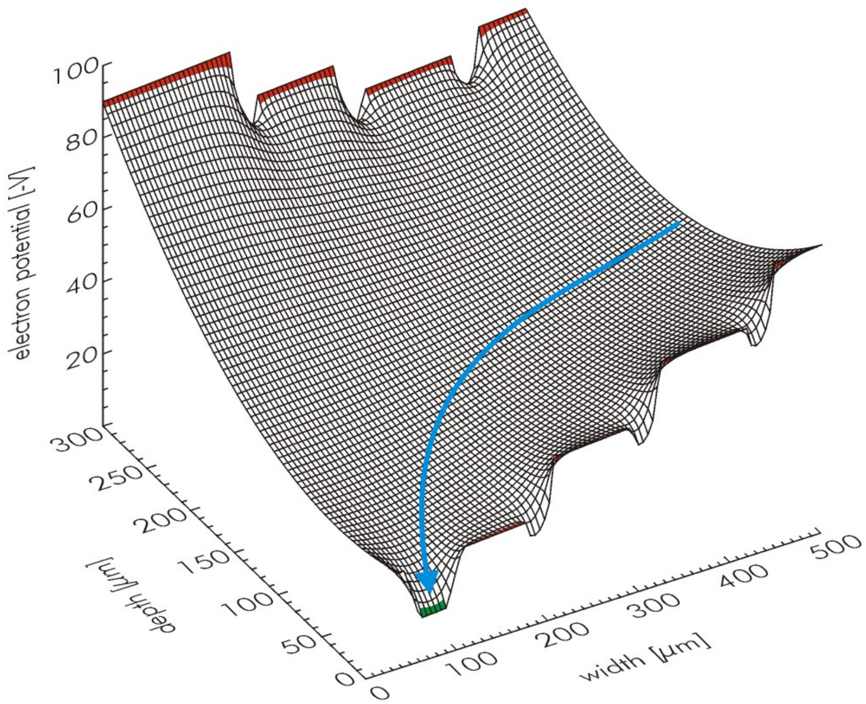


2D position resolution by

- drift time measurement
- segmentation of the anode

# Drift detector: signal shape
## (first measurements by Rehak and Holl, 1985)

PNSensor

## Signal for varying distance

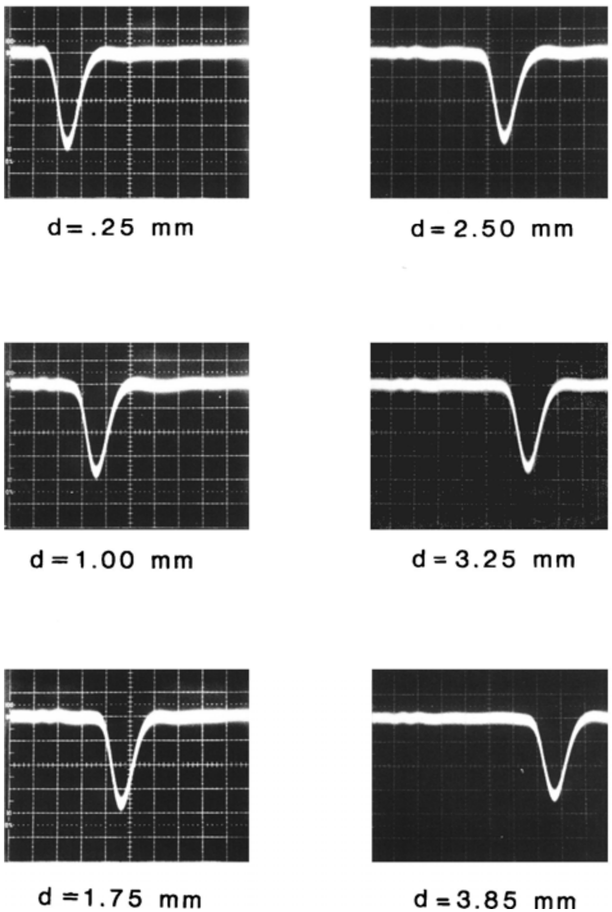


## for varying drift field

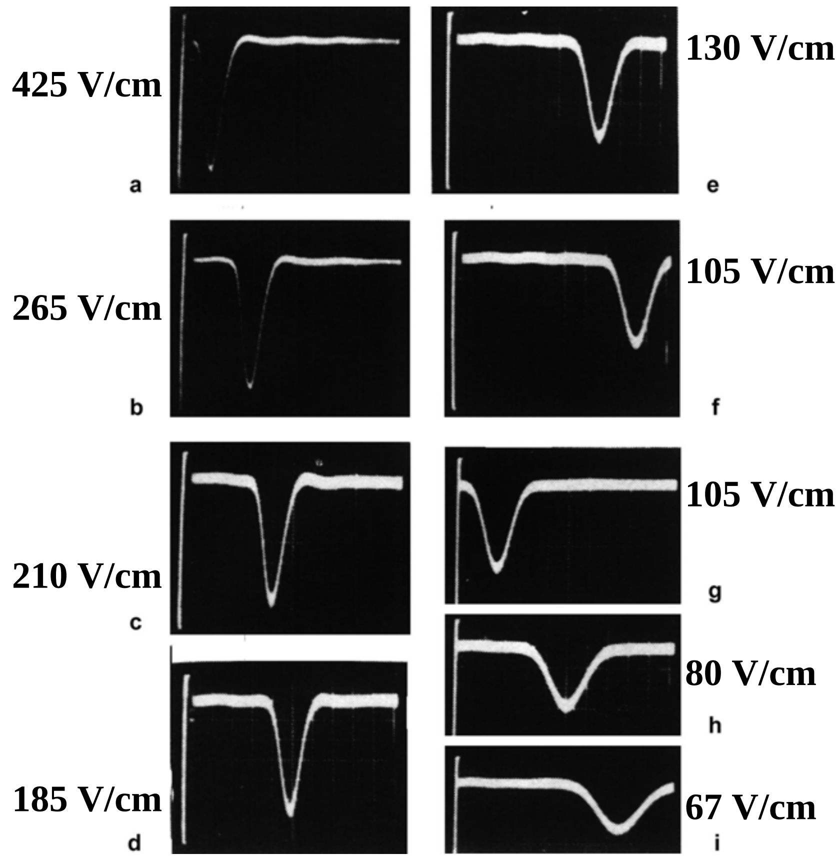


**Light pulser 22000e** **200 ns/div** **Light pulser 22000e**

# Integrated electronics on high resistivity Silicon

$$ENC^2 = \left(\alpha \frac{2kT}{gm} C^2_{tot} A_1\right)\frac{1}{\tau} + \quad \text{serial noise}$$

$$+ \left[\left(2\pi a_f C^2_{tot} + \frac{b_f}{2\pi}\right) A_2\right] + \quad \text{low frequency noise (e.g. 1/f)}$$

$$+ \left(q I_l + \frac{2kT}{R_f} A_3\right)\tau \quad \text{parallel noise}$$

because of Q = C · U

ΔU = ΔQ / C

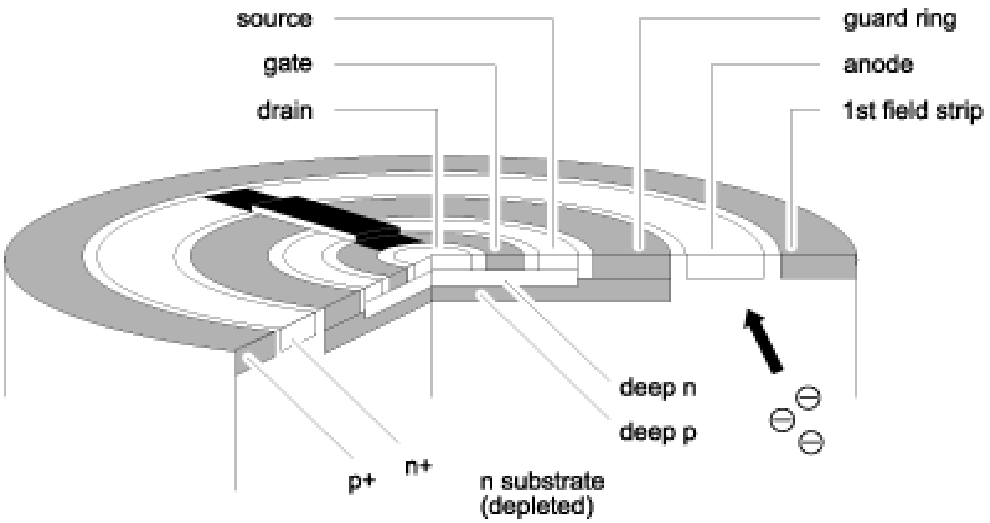

# SDDs for astrophysics and industrial applications

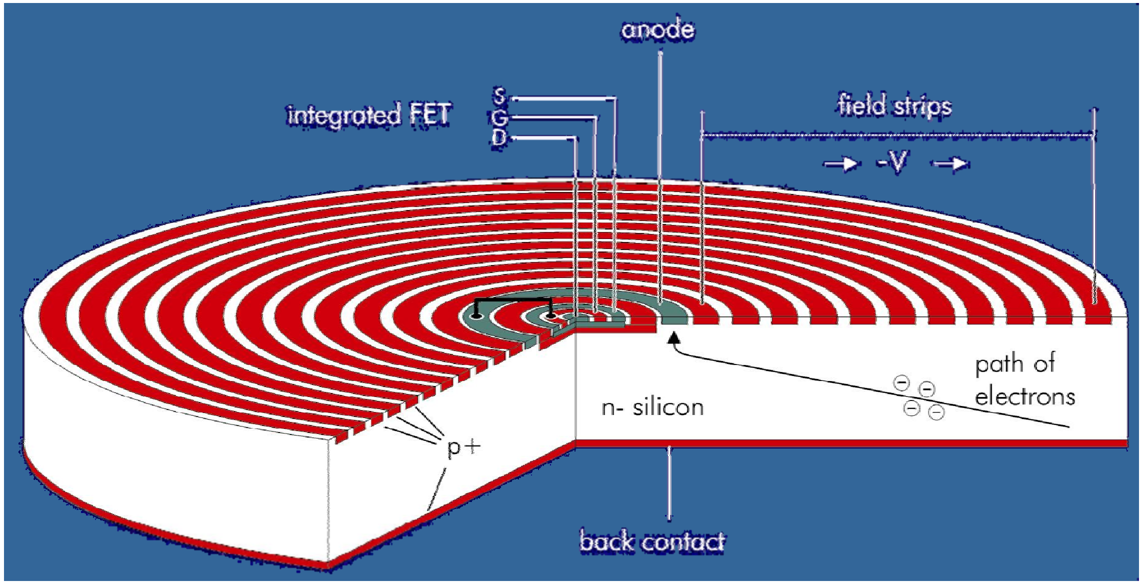


**SDD with integrated SSJFET**

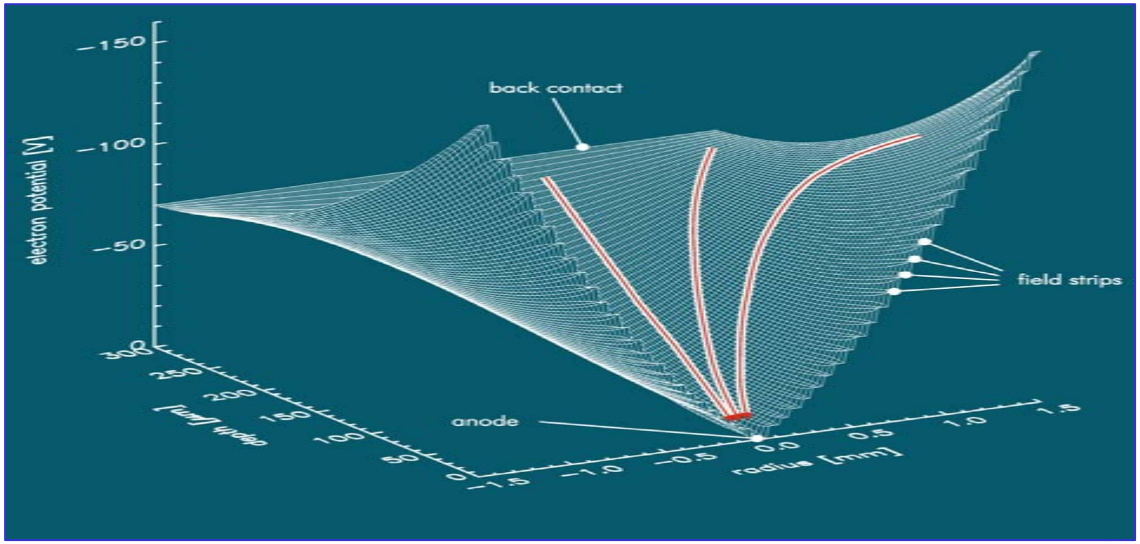


**Electrical Potential in a circular SDD**

# SDD properties

- •Energy resolution: $\Delta E_{FWHM}$ = 125 eV
- •Count rate capability: up to $10^6$ cps
- •Peak/Background ≈ 10.000 : 1
- •Quantum efficiency: > 90% @ 0.3-10 keV
- •Rad. hardness: > $10^{14}$ $Mo_K$ Photonen
- •Operating temperature: T ≈ - 10° C
- •Random shape and size

- •Triggersignal: $\Delta t$ ≈ 3 – 5 ns
- •Antireflective coating

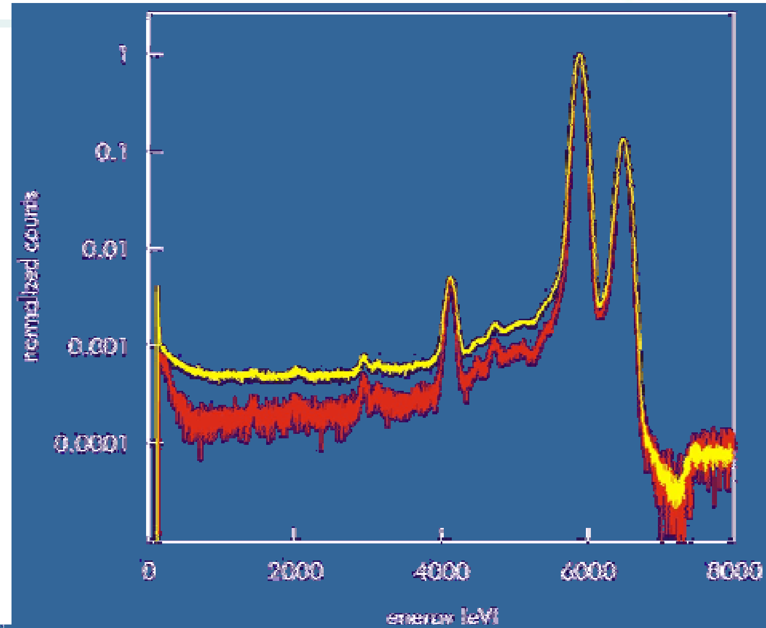


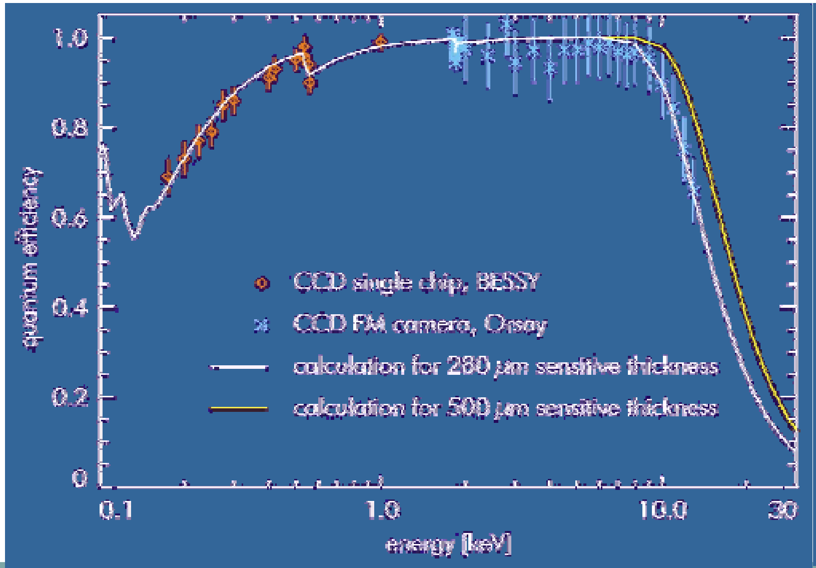


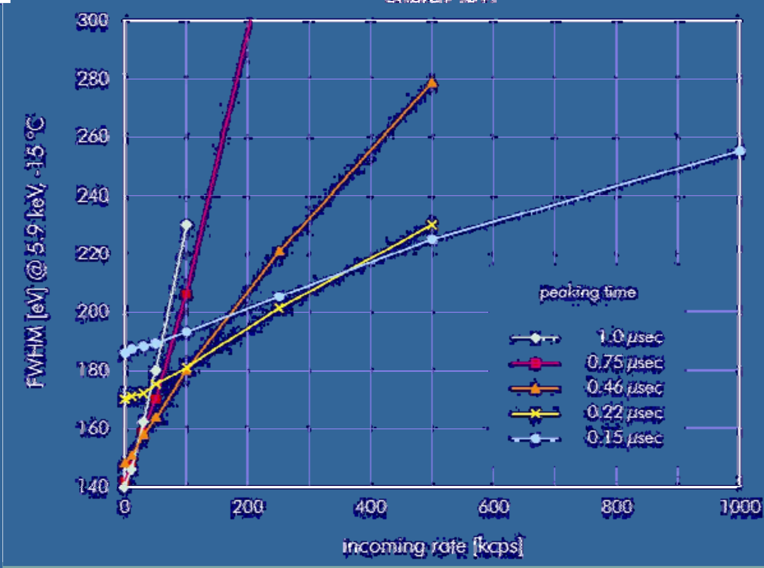

# Applications of SDDs

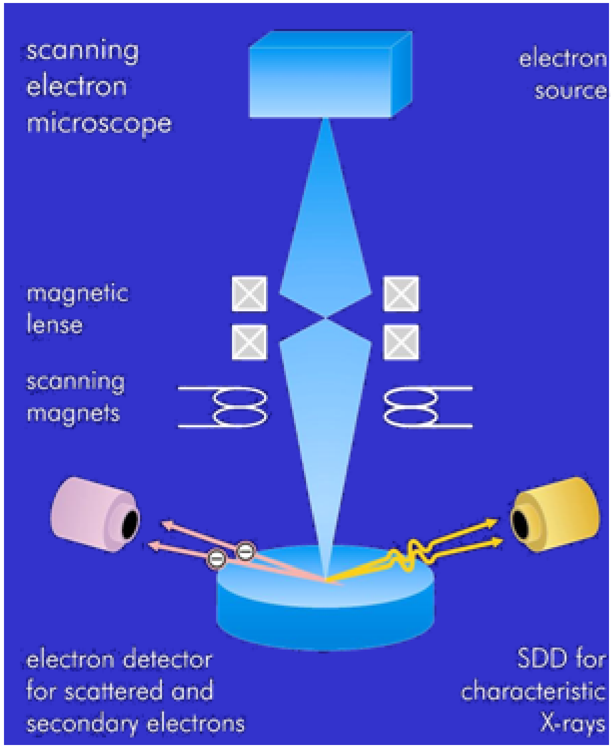


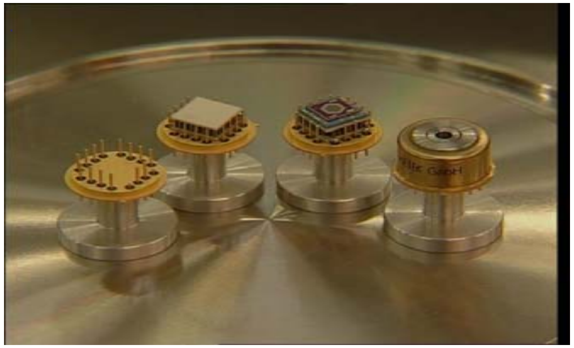

**SDD – Modules from $5\ mm^2$ bis $100\ mm^2$, 1 – 61 Module/Chip**

**Measurements made by RÖNTEC, Berlin**

**SEM – image**

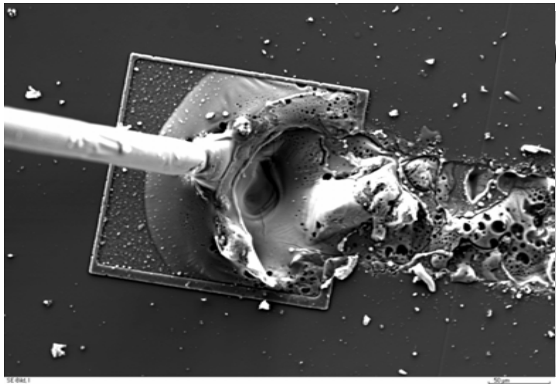

**Scanning electron microscope with separated electron and X-ray detector**

**``colour – image´´**

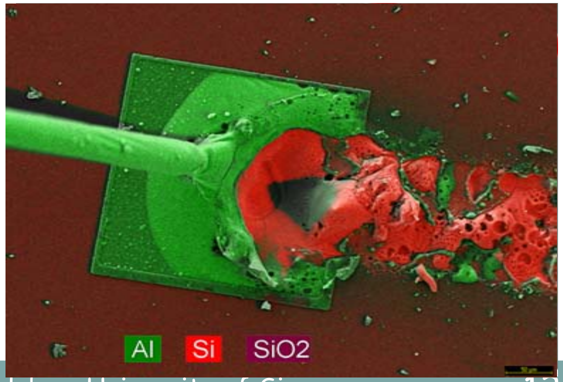

# Applications – XRF in Art Analysis

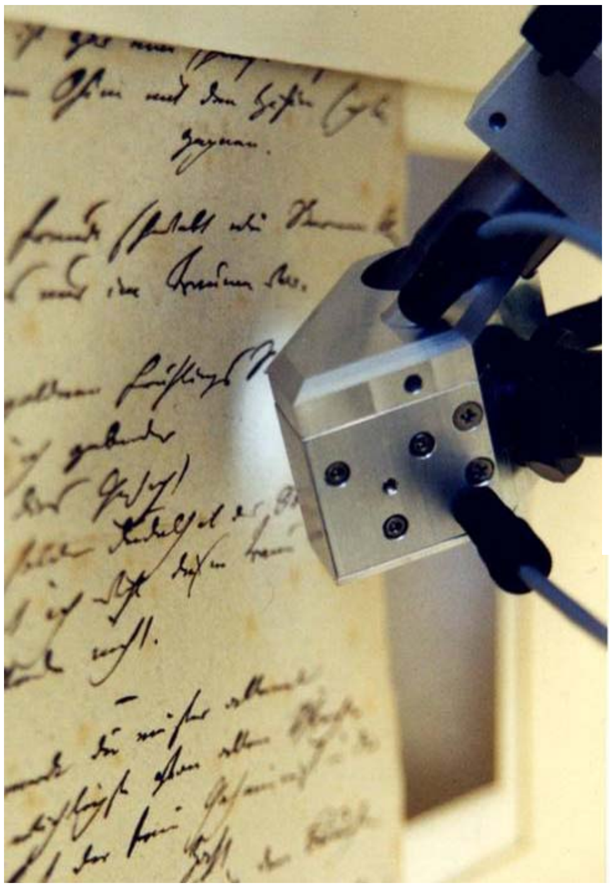

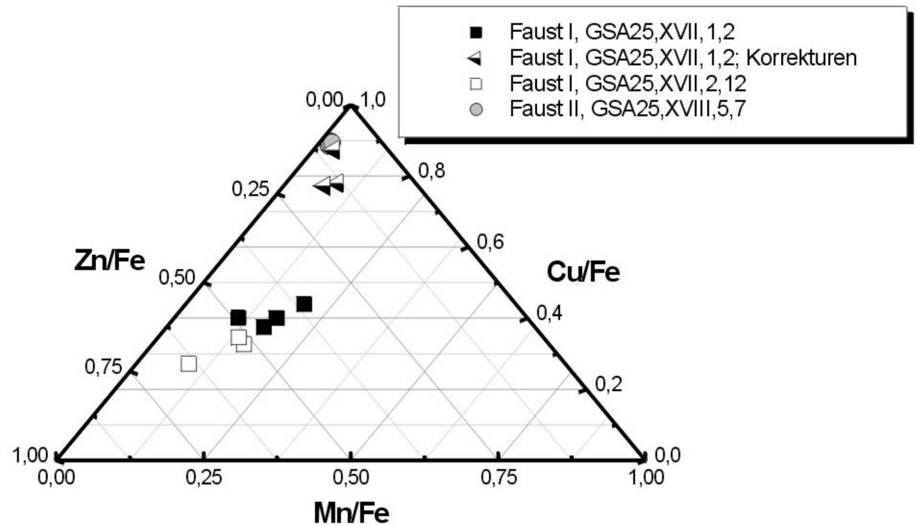


"fingerprint" of Goethe's ink

⇒ editing of Faust I during Faust II work

experiment & figures by O. Hahn (BAM, Berlin)

with portable system "artTAX" (RÖNTEC)

# Mars Exploration Rover (MER)

**mission profile**

- 2 independent mobile landers “Spirit” & “Opportunity”
- arrived 04./25.01.04
- scheduled for 3 months / 600 m but still active

**mission goals**

- find traces of water
- investigate the geology of Mars
- prepare manned mission

PI of APXS system: R. Rieder
MPI für Chemie, Mainz

# APXS (Alpha Particle X-ray Spectrometer)

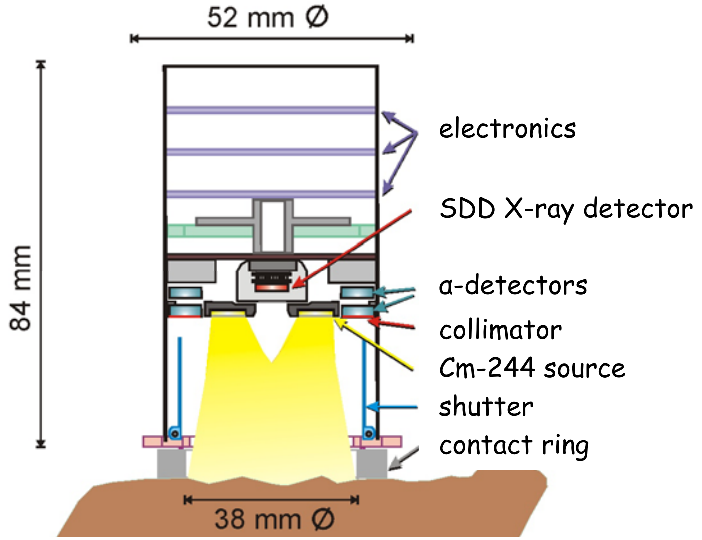


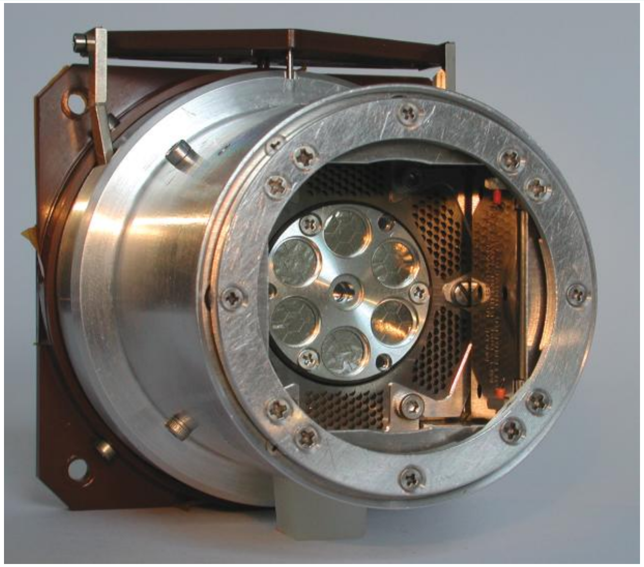

- Curium-244 α- and X-ray sources
- Silicon Drift Detector
  - PIXE, XRF
- α-particle detectors
  - Rutherford backscattering

similar system on board of the ROSETTA comet lander

# Results of SDD measurements on Mars

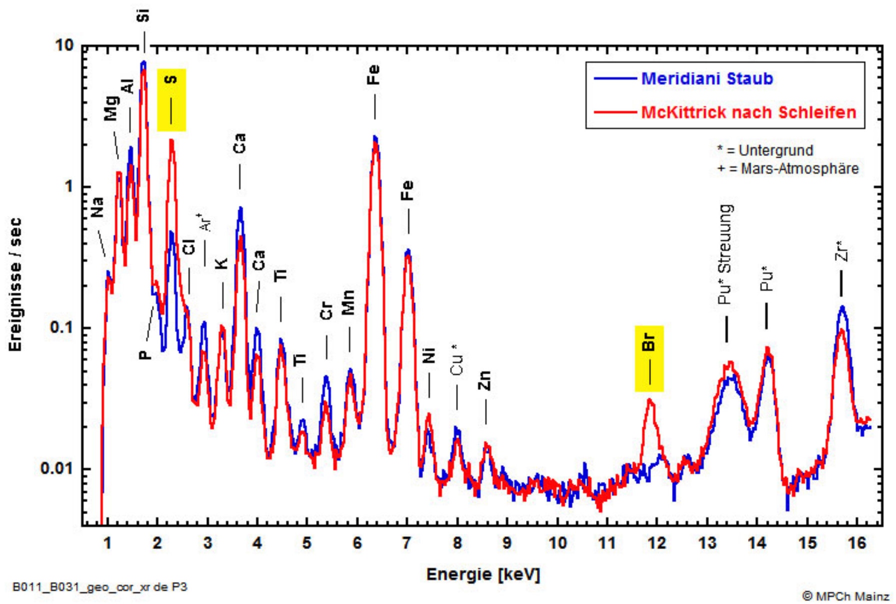


**SDD**

X-ray spectra of Marsian samples (2004)

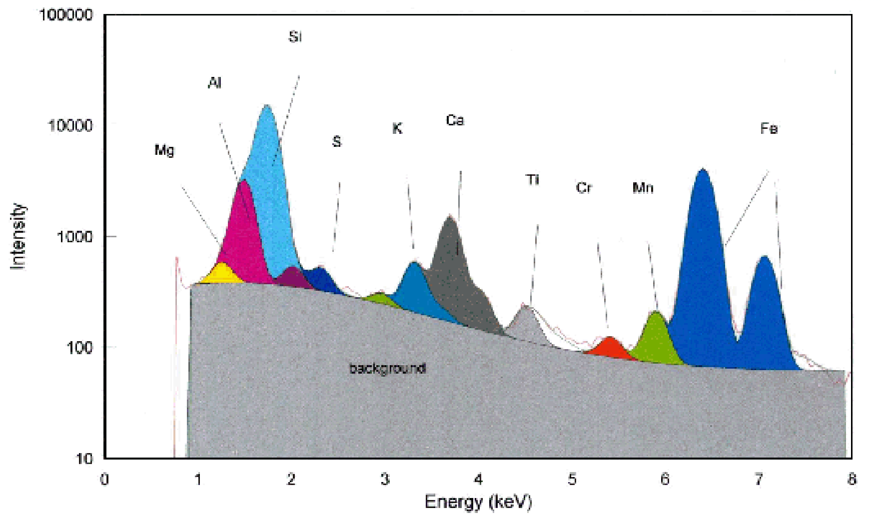


for comparison:

X-ray spectrum of Marsian sample

by Pathfinder mission (1997)

equipped with **PIN-diode**

# Multichannel SDD applications

## scintillator readout, medical γ-ray imaging

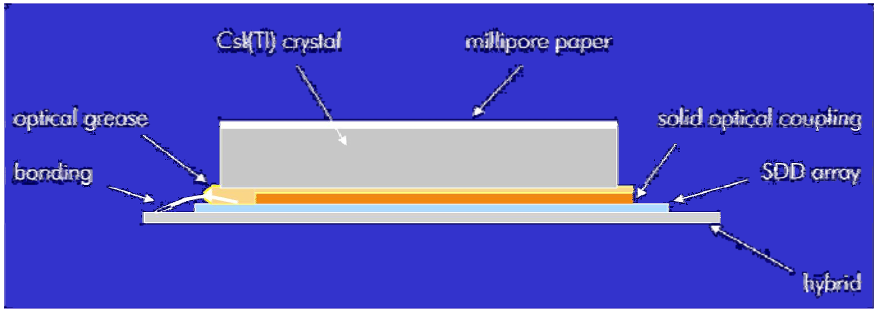


- CsI(Tl), 3mm
  η = 80 % (122 keV)
- gain
  15.4 el./keV
- position resolution
  0.35 mm FWHM
- energy resolution
  17.4 % FWHM
  E(min) = 2 keV

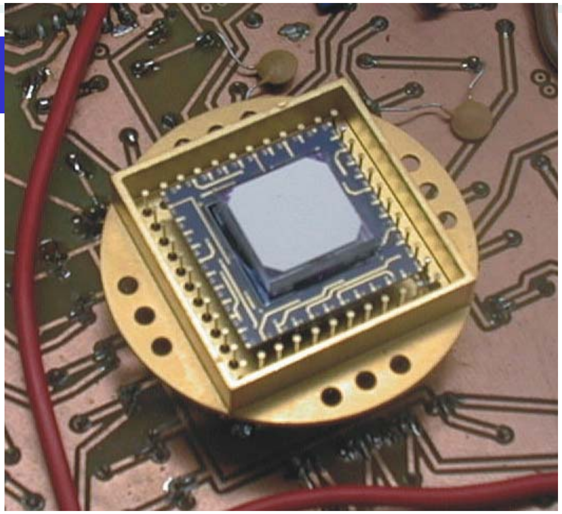

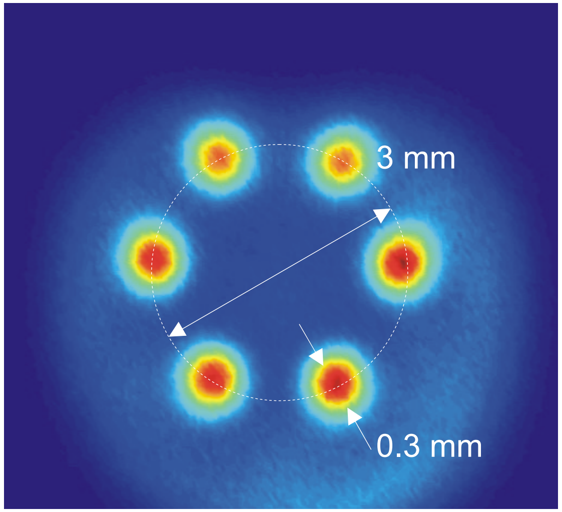


experiment & figures by C. Fiorini, Politecnico di Milano

# Spectroscopic response of SDDs coupled to scintillators

Measurements by C. Fiorini, A. Longoni, Politecnico di Milano

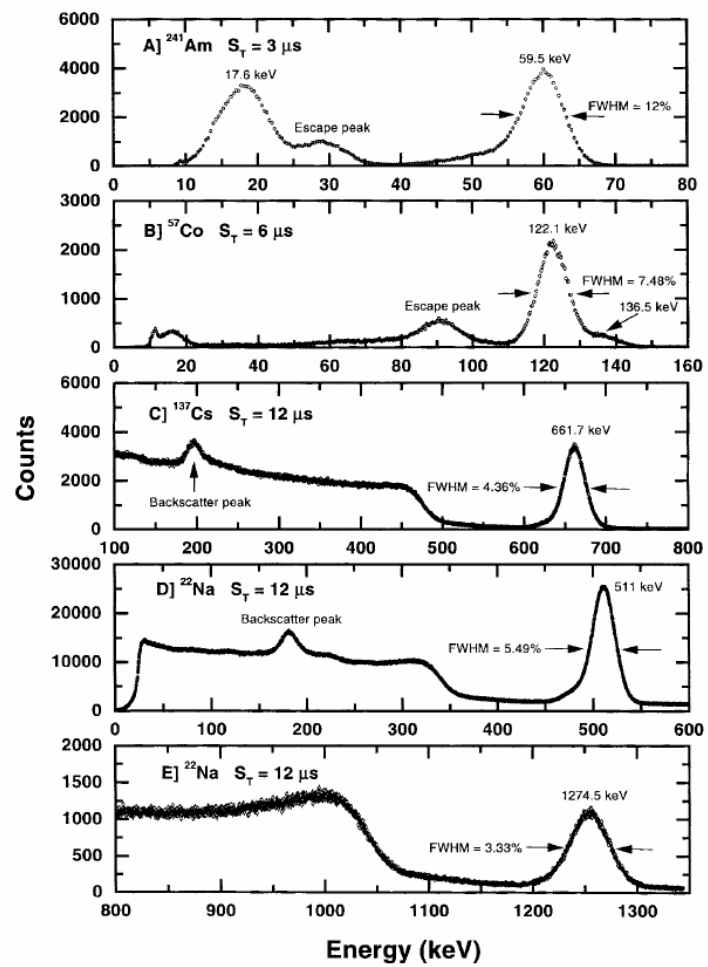


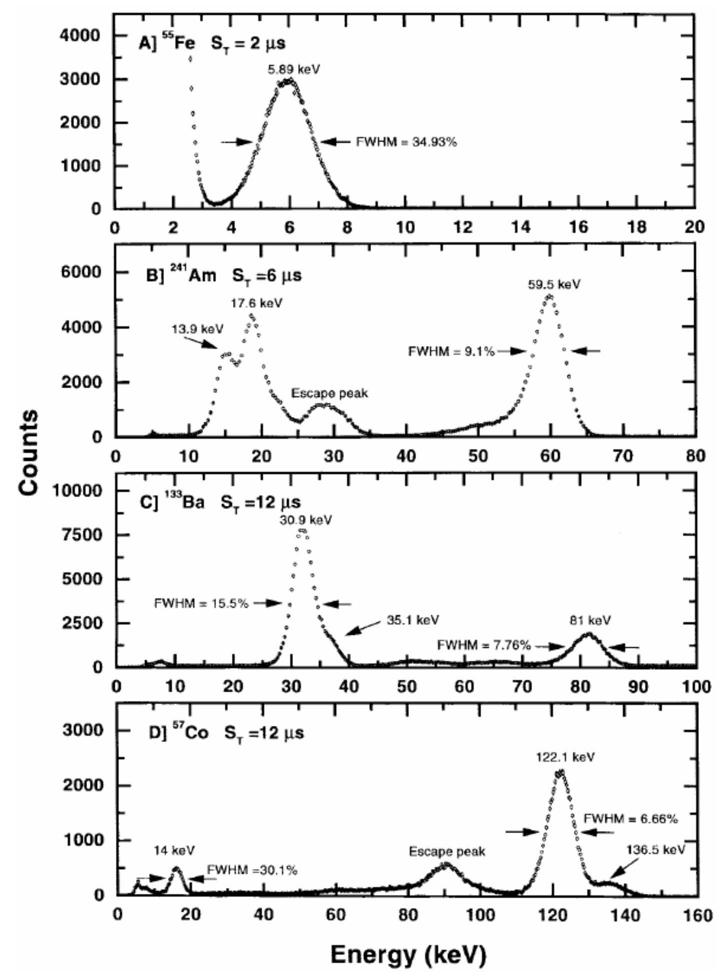

# From SDDs to CCDs

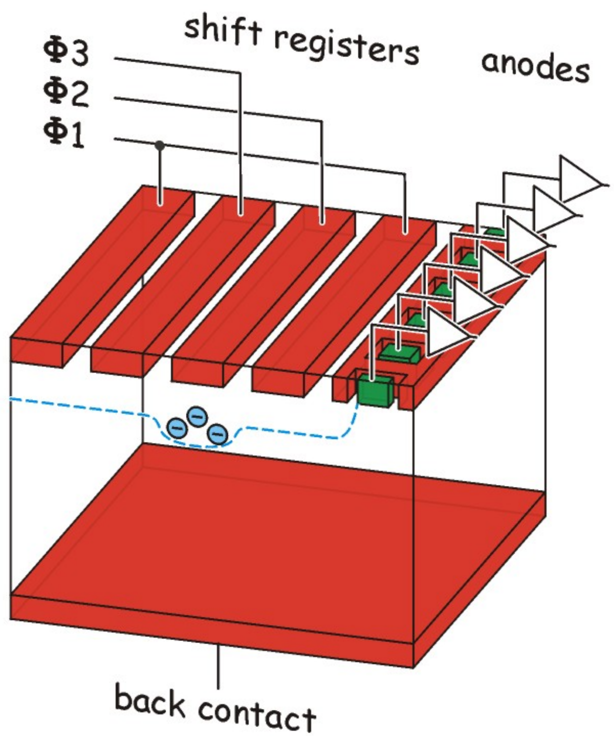


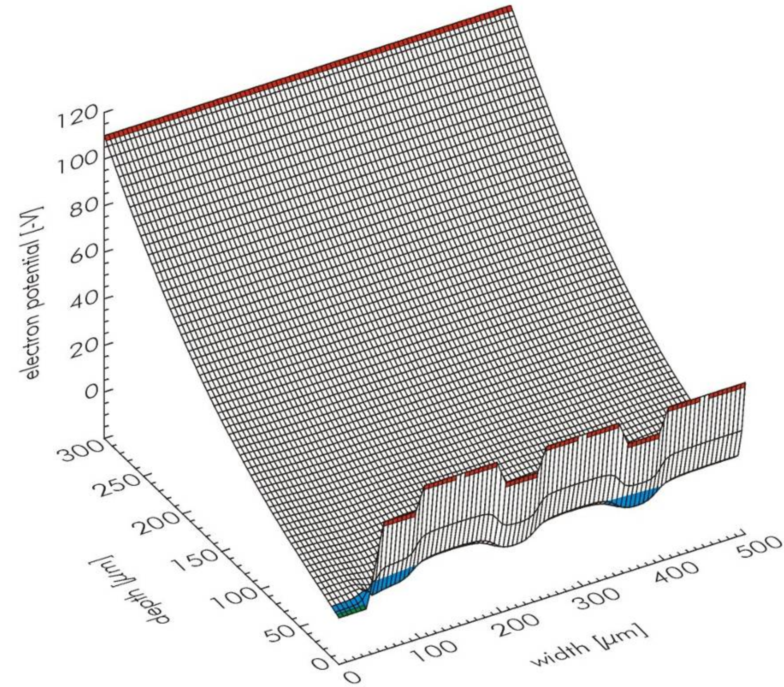


- full depletion (50 µm to 500 µm)
- back side illumination
- radiation hardness
- high readout speed
- pixel sizes from 30 µm to 1 mm
- charge handling: more than $10^6$ $e^-$/pixel
- high quantum efficiency

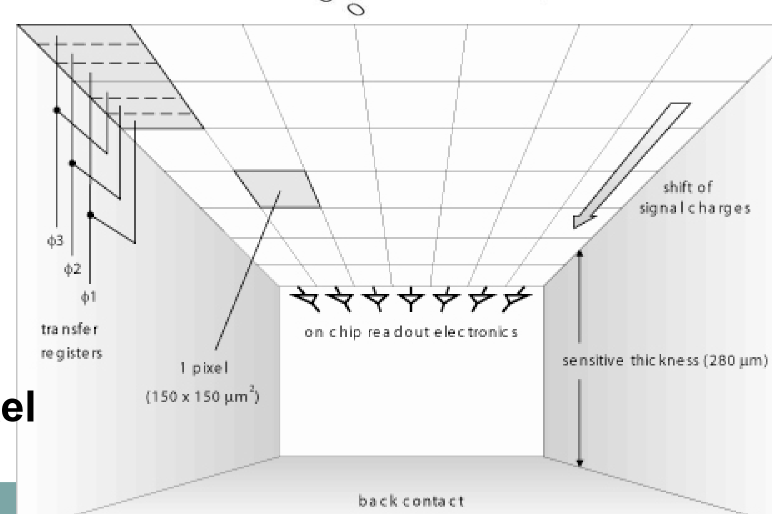

# Charge transfer in the pnCCD

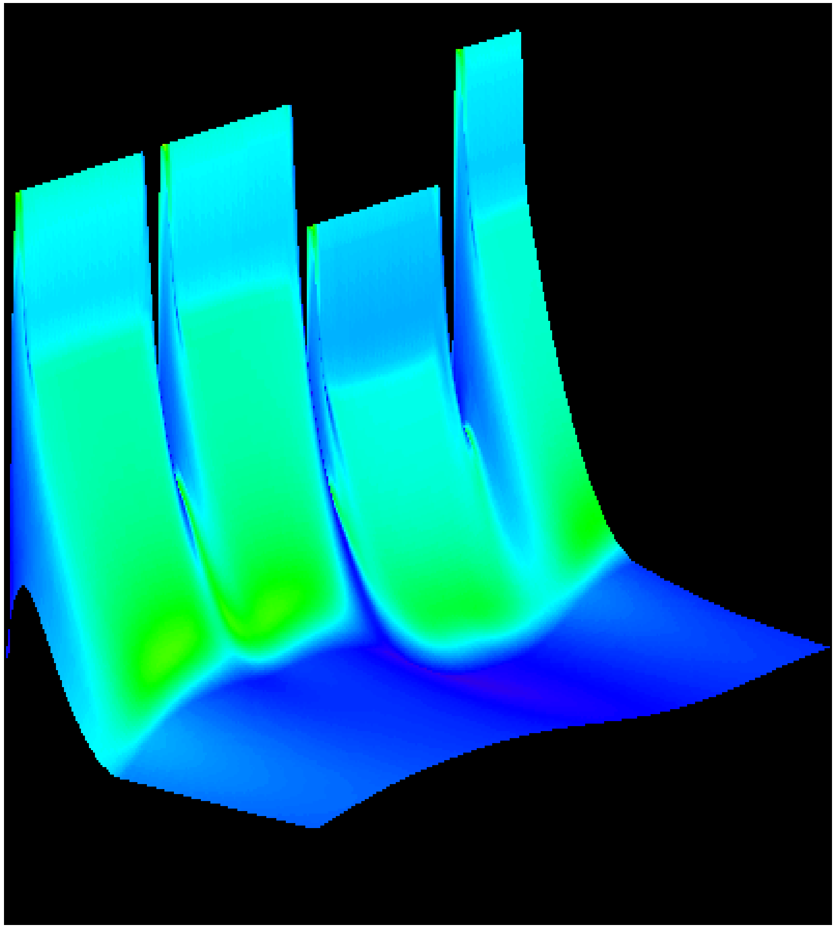

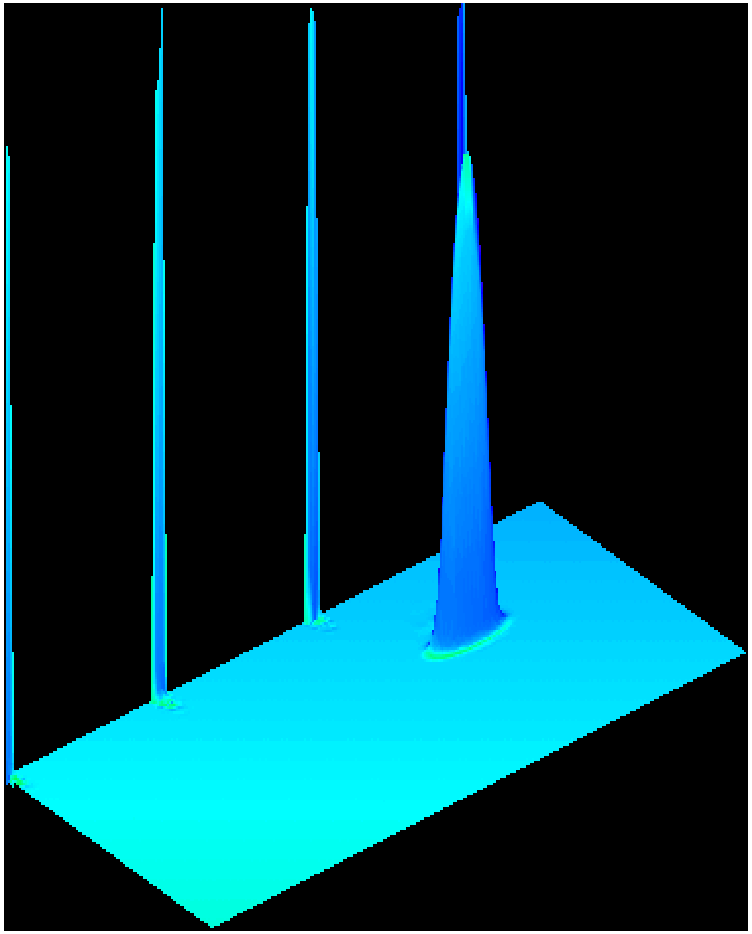

# XMM – Newton launched on 10.12.1999

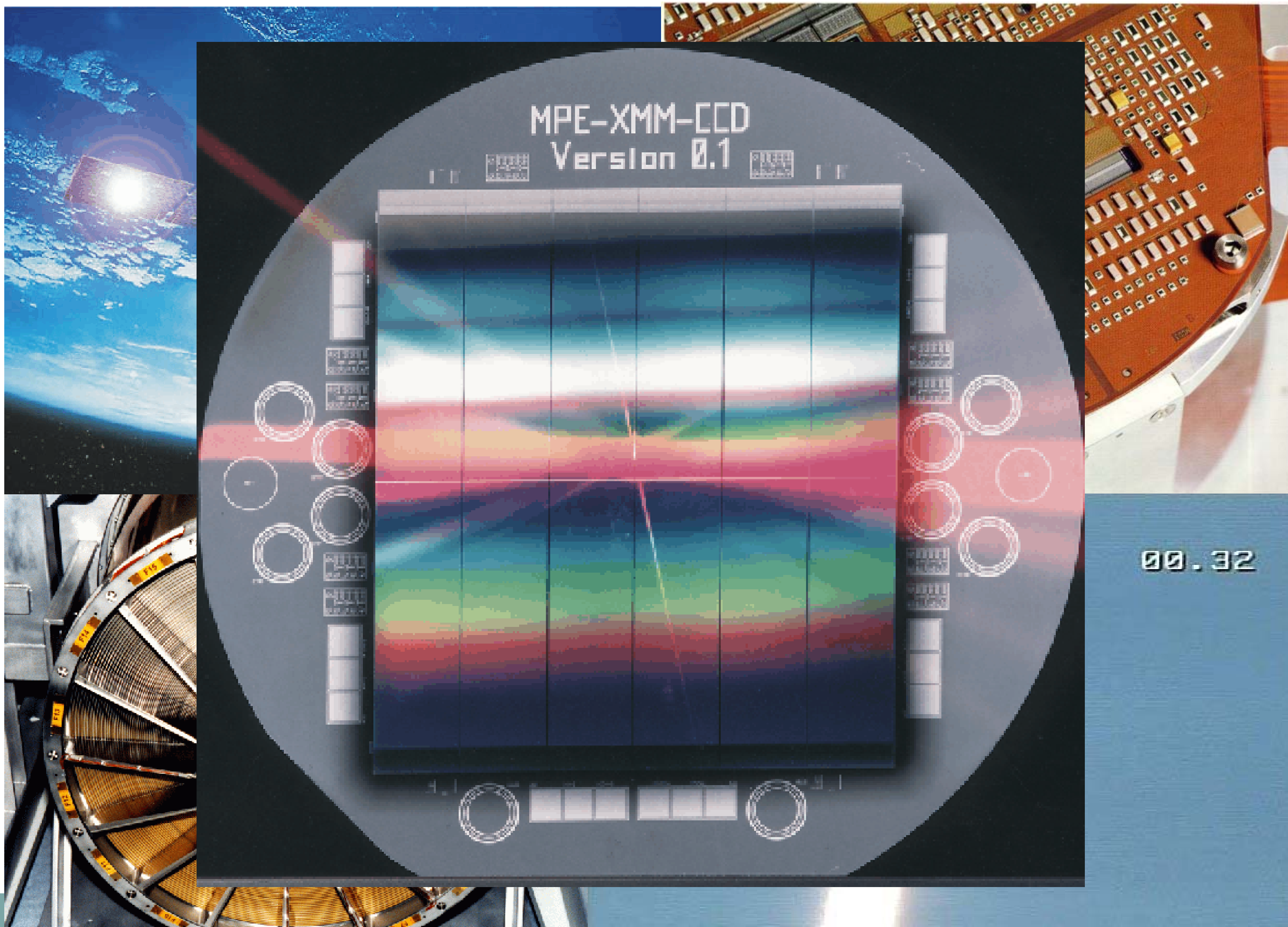

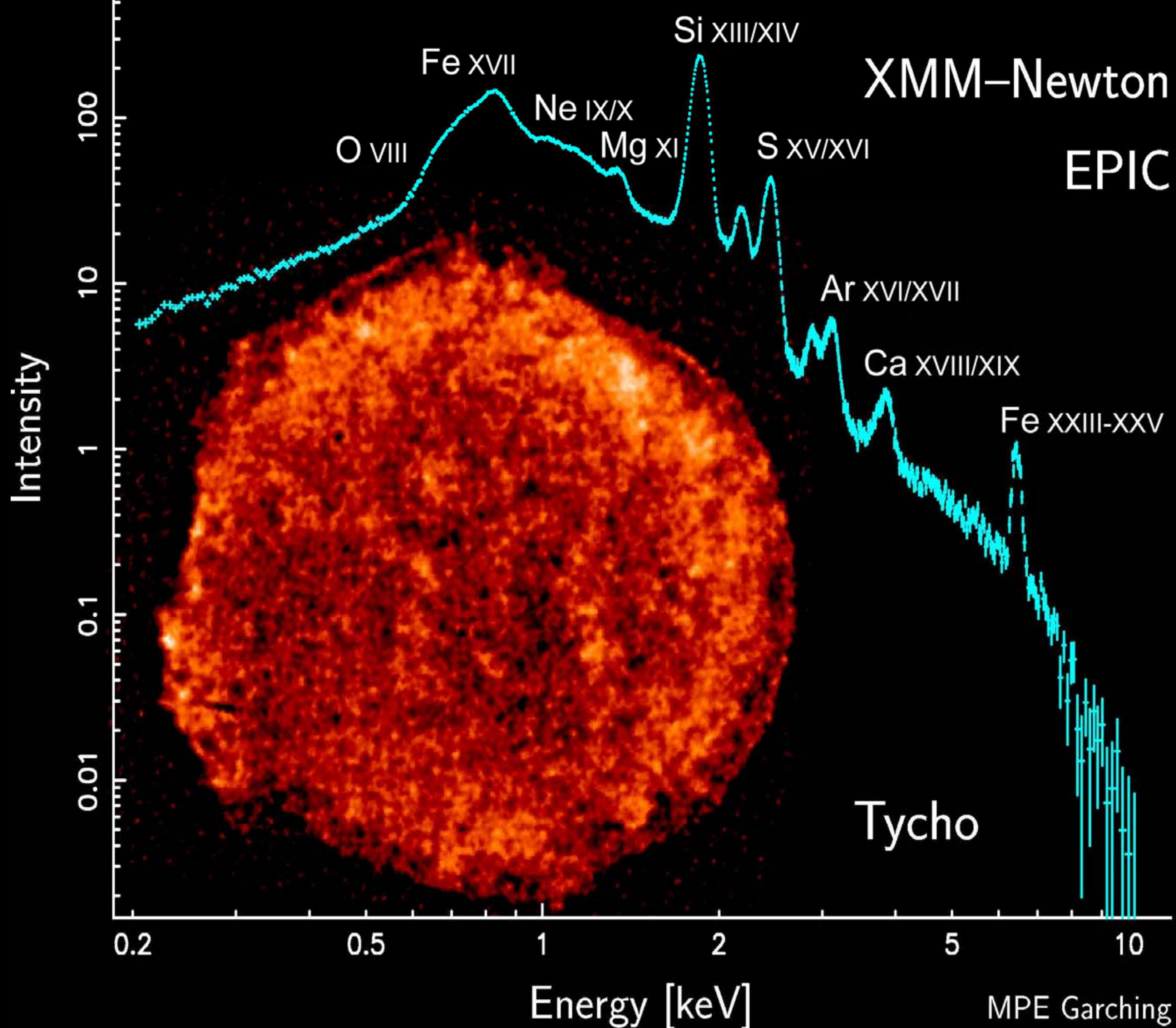

XMM–Newton
EPIC
Si XIII/XIV
Fe XVII
Ne IX/X
Mg XI
O VIII
S XV/XVI
Ar XVI/XVII
Ca XVIII/XIX
Fe XXIII-XXV
Tycho
Intensity
100
10
1
0.1
0.01
0.2
0.5
1
2
5
10
Energy [keV]
MPE Garching

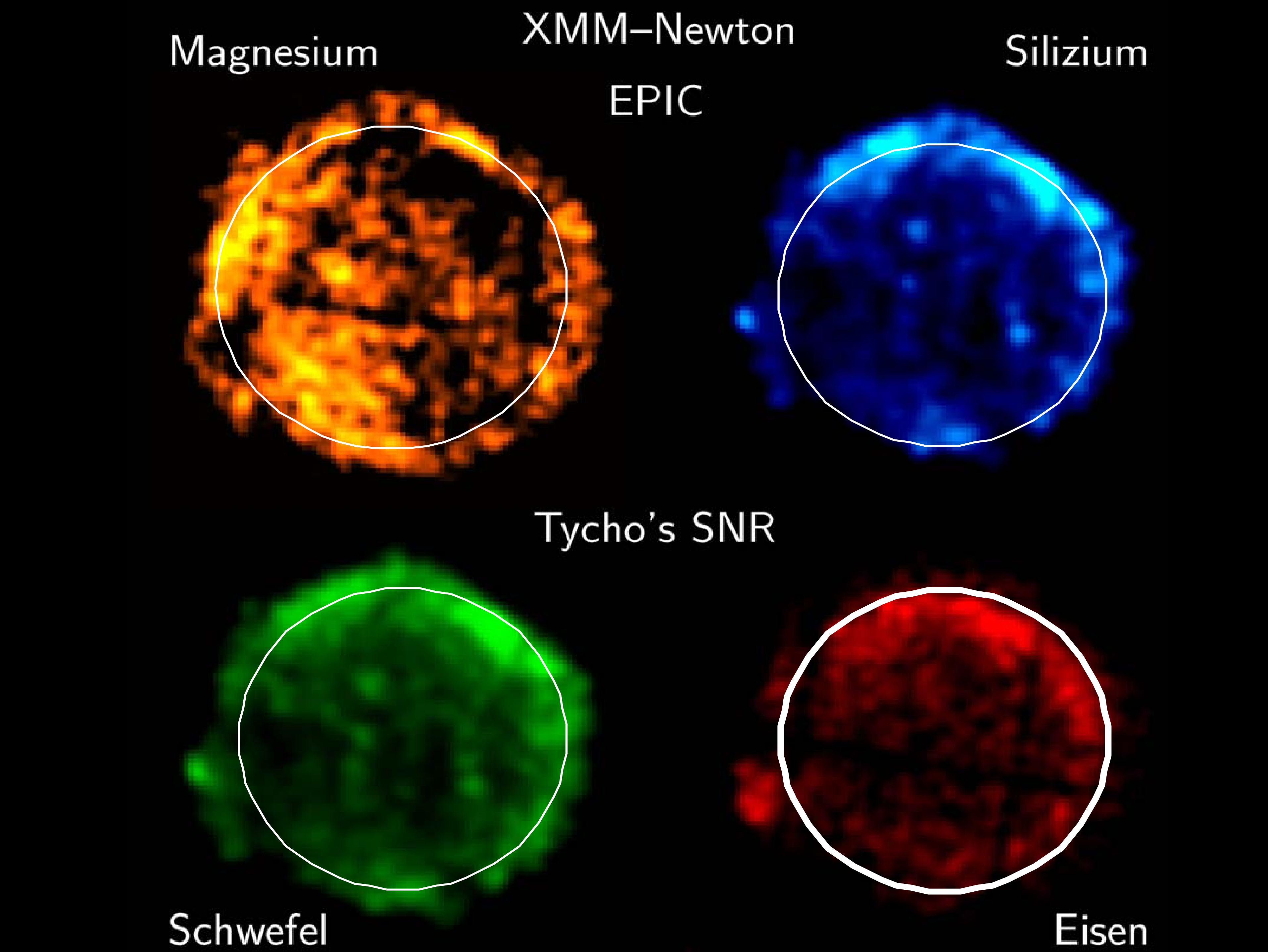
XMM–Newton
EPIC
Magnesium
Silizium
Tycho's SNR
Schwefel
Eisen

# Gamma ray burst afterglow observation with XMM

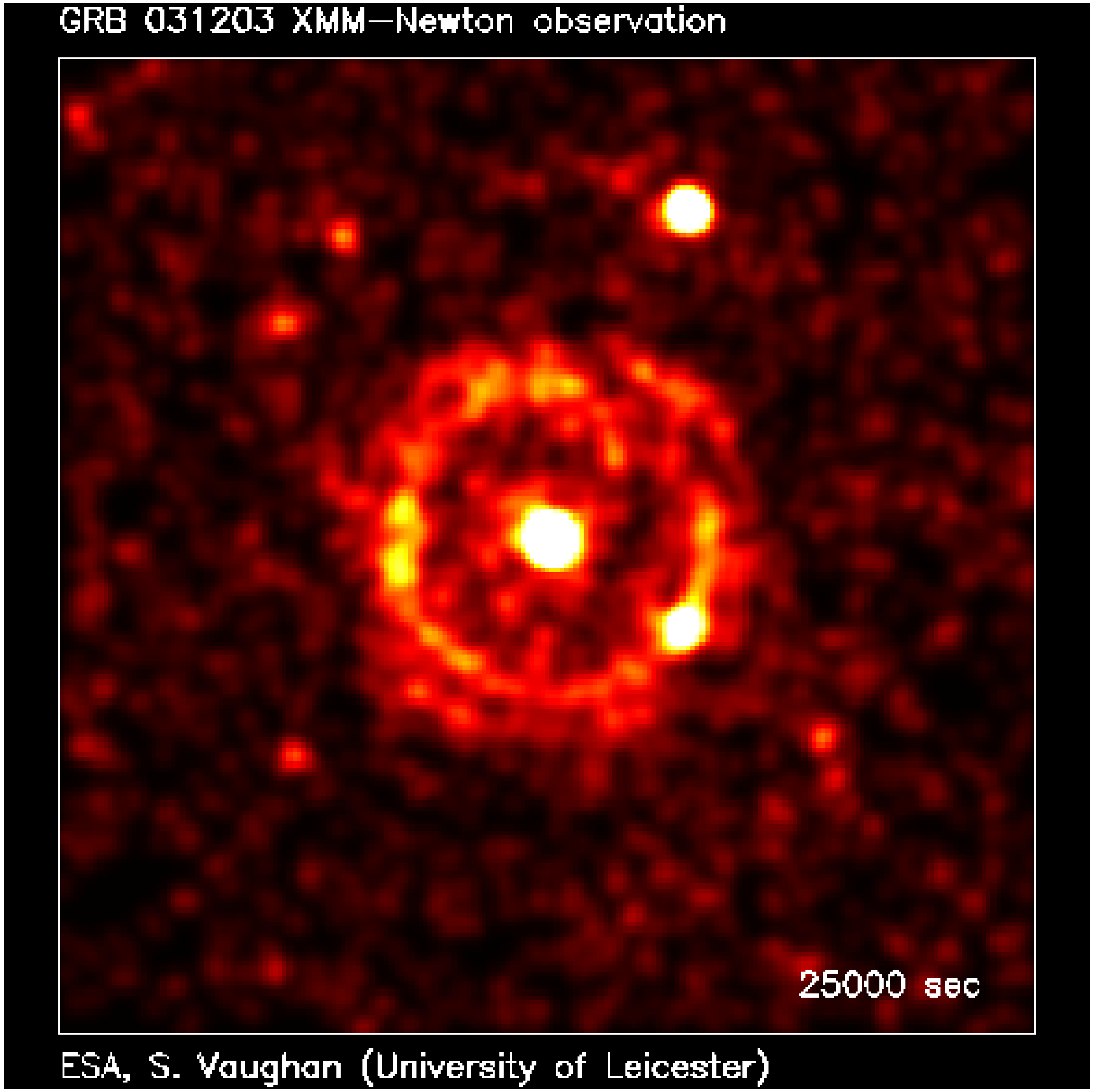

# Head-on collision of clusters of galaxis observed with XMM

model of the ``cosmic thunderstorm´´

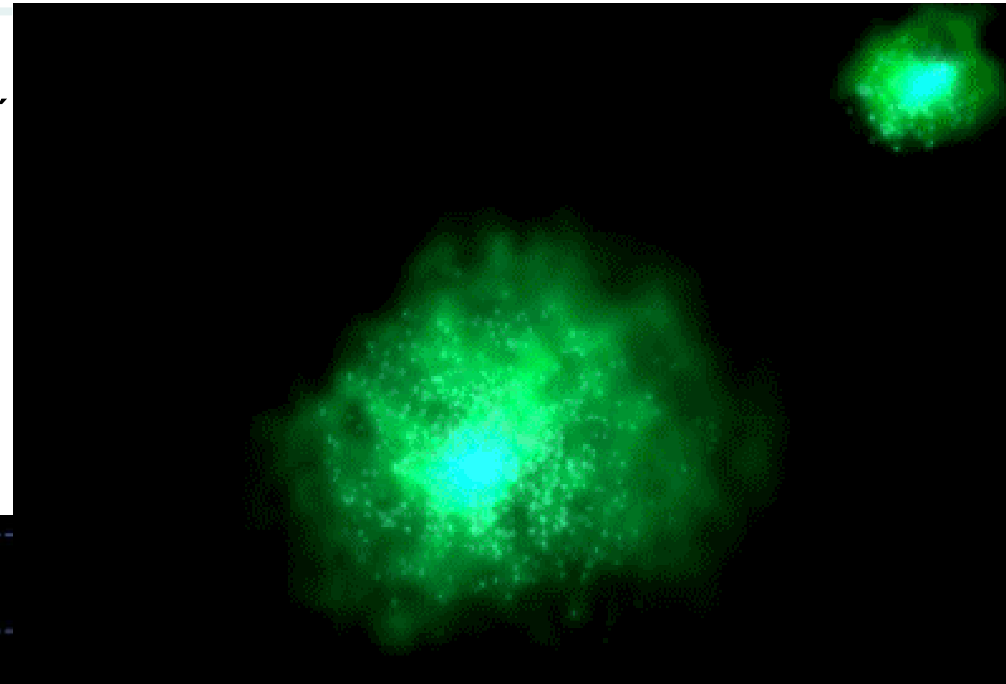

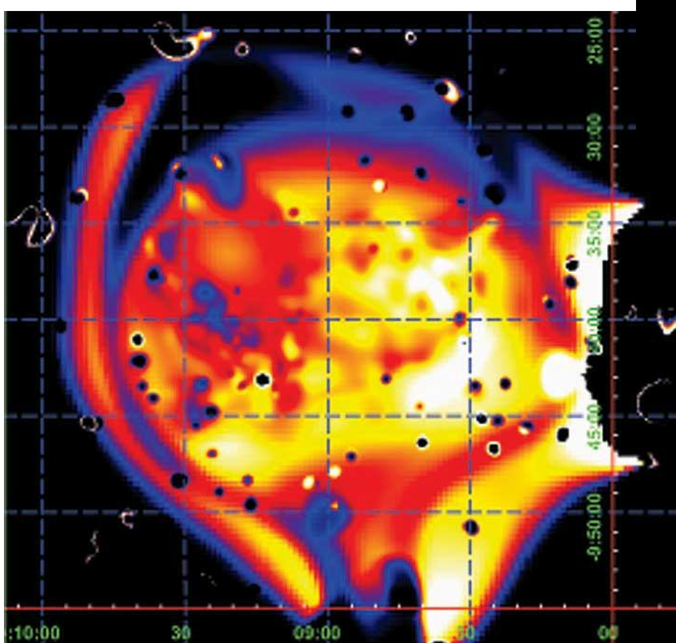


measured temperature and density maps from XMM – Newton of Abell 754

# XMM Summary

1. Working since launch
(10. Dez. 1999)
without any problem.
2. The energy resolution @ the $Al_K$ line (1.5keV) decreased since launch from 98 eV to 99 eV (FWHM).
3. Since launch the operating conditions have never been changed.
4. Up to now about 6000
observations were made with XMM – Newton.
In 80 % of all observations the pnCCD was chosen as `prime instrument´.
5. Up to now, 900 refereed astrophysics papers have been published

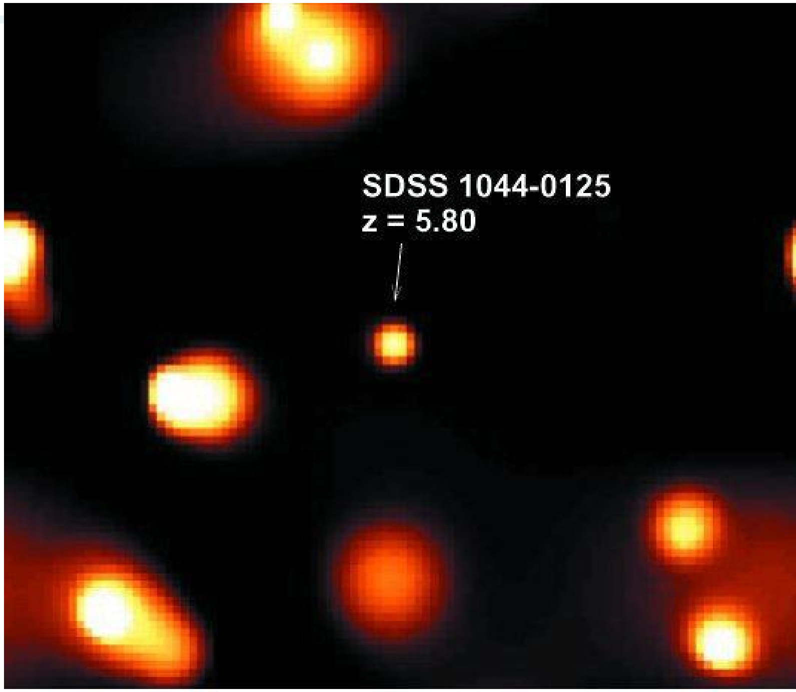

QSO SDSS 1044-0125
European Space Agency

# High speed frame store pnCCDs for X-rays, UV light, visible and near infrared light

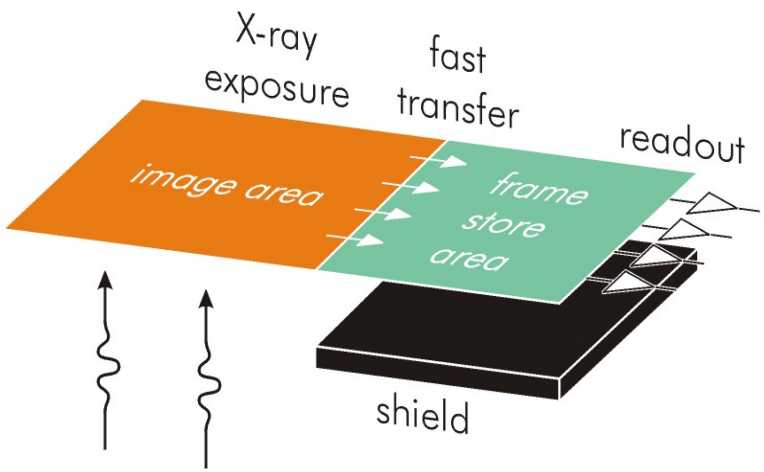


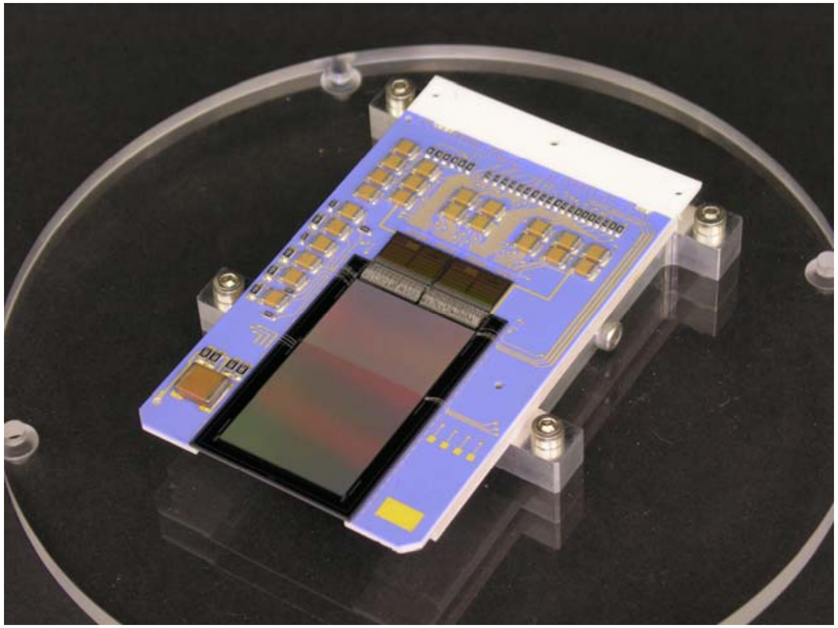

**FS pn-CCD for the ROSITA mission (ESA, DLR, RSA)**

- **format** 256 x 256
- **pixel size** 75 µm □ image
  50 µm □ frame store
- **out-of-time** 0.1 %

# III. Performance: spectroscopy Fe55

C11_11_61_050422_01, T = -83°C; 54 ms

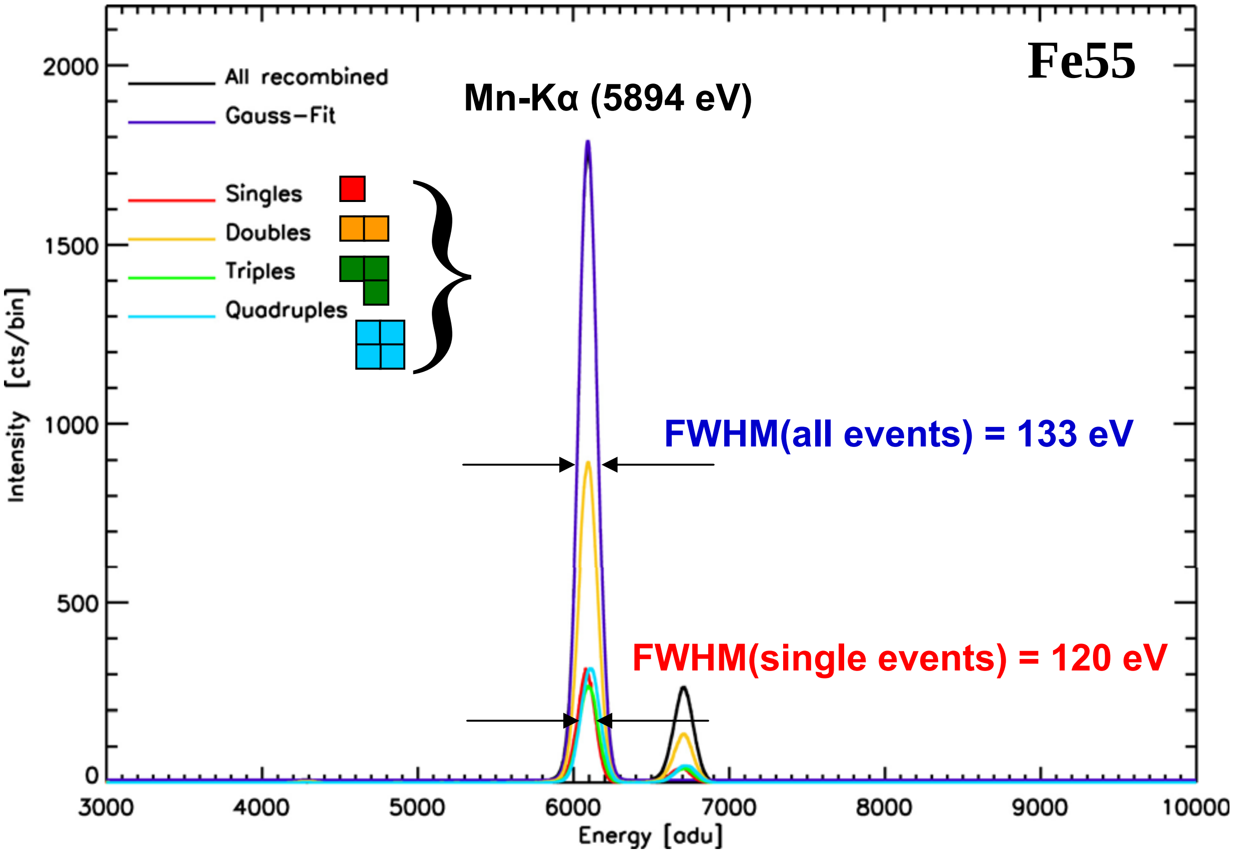

# III. Performance: spectroscopy 277 eV

C11_11_25_050512_02

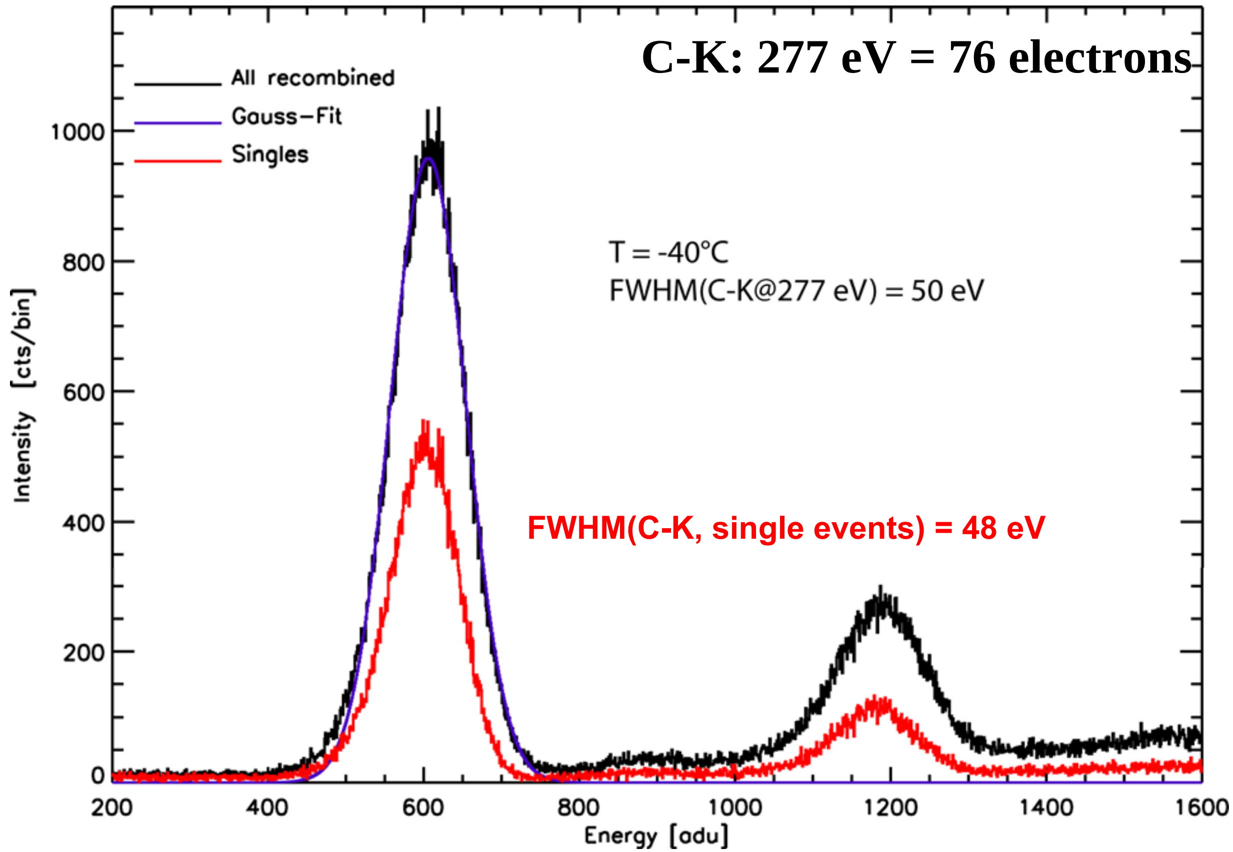

# Optical properties of the pnCCD

150 mm wafer of recent CCD fabrication

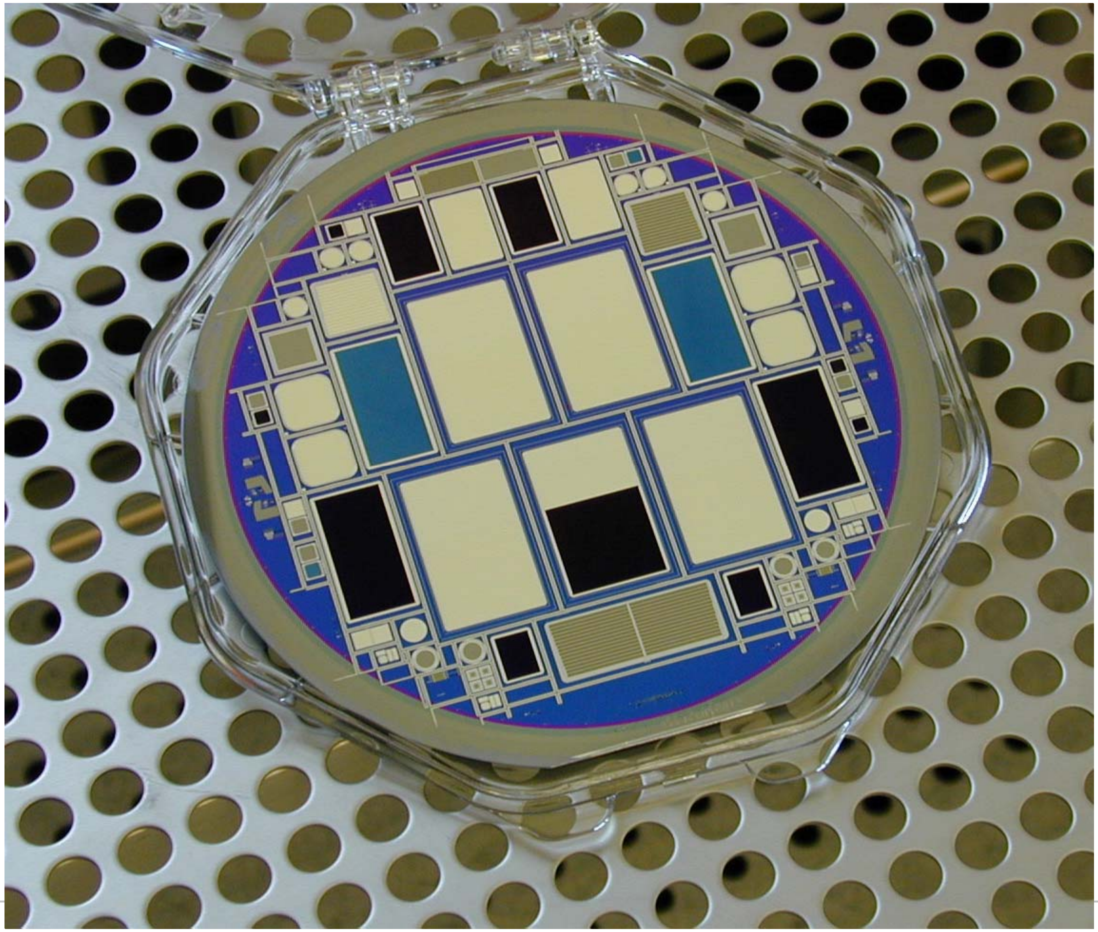

# 51mm pnCCD with a double-sided readout, mounted onto a ceramic substrate

MPE PNSensor

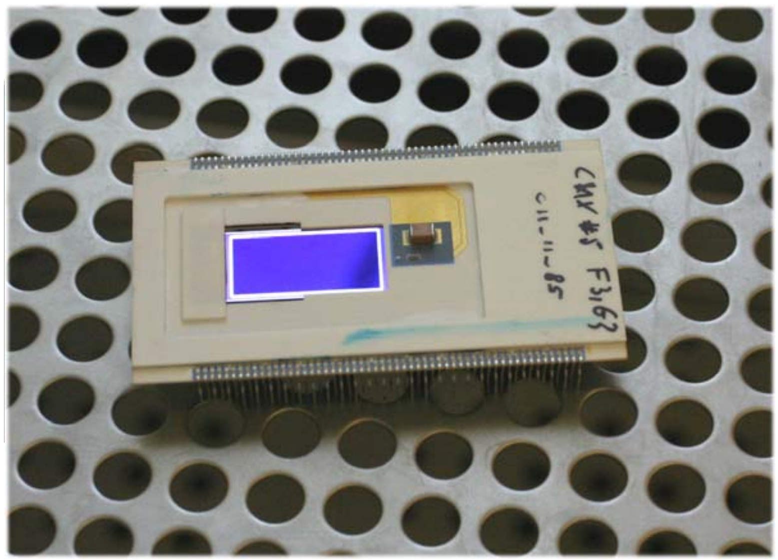

- detector size = $27 \times 13.5$ mm$^2$
- 51 µm □ pixel size
- $528 \times 264$ pixel in total,
  $132 \times 264$ in each image & storage area
- readout transfer to both sides
- image transfer time = 30 µs
- OOT probability = 3% @ 1000 fps
- charge transfer loss CTI ≈ $10^{-5}$
  i.e. total charge loss < 0.15 %
- charge handling capability > $10^5$ $e^-$
- 100% fill factor
- readout noise vs. frame rate:
  - 1.8 $e^-$ @ 10 .. 400 fps
  - 2.3 $e^-$ @ 400 .. 1.100 fps
- With binning:
  - 2.3 $e^-$ @ 2.200 .. 4.400 fps

# System configuration

## CAMEX amplification- and readout-chip

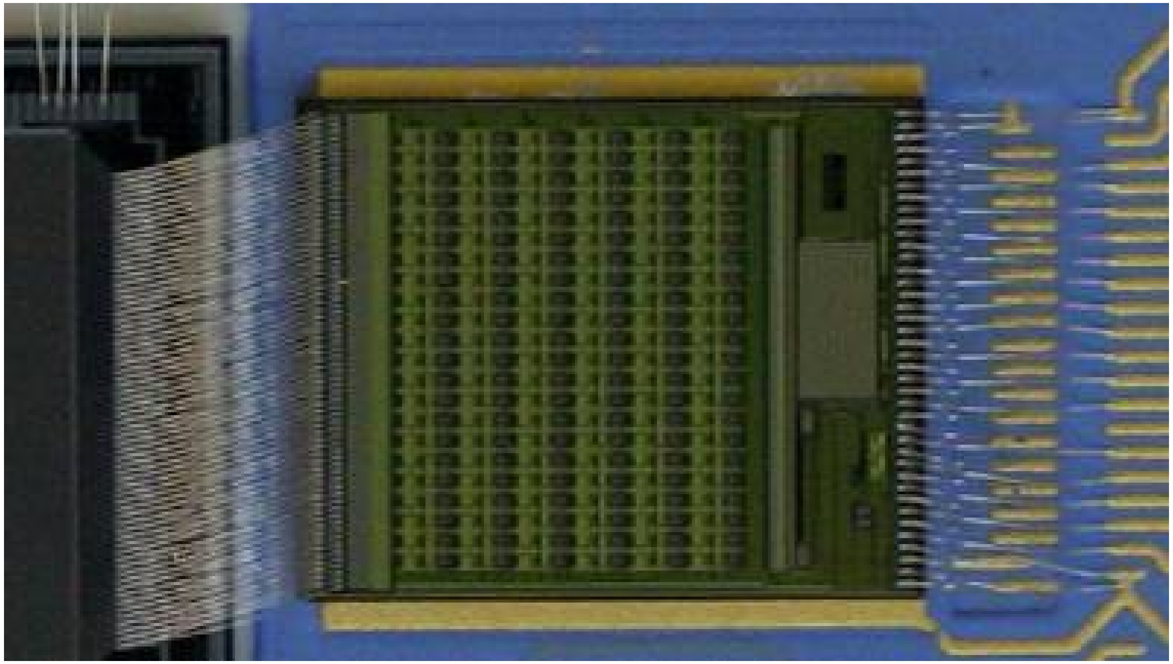

- Multi-correlated double-sampling filtering (MCDS)
- Signal processing of all channels in parallel (132)
- Selectable gains and operating modes
- Electronic noise contribution less than 1 $e^-$
- Readout-speed per node up to 10MHz (i.e. 6.6$\mu$s per line on two readout nodes)

# Optical properties of the pnCCD

## Internal quantum efficiency

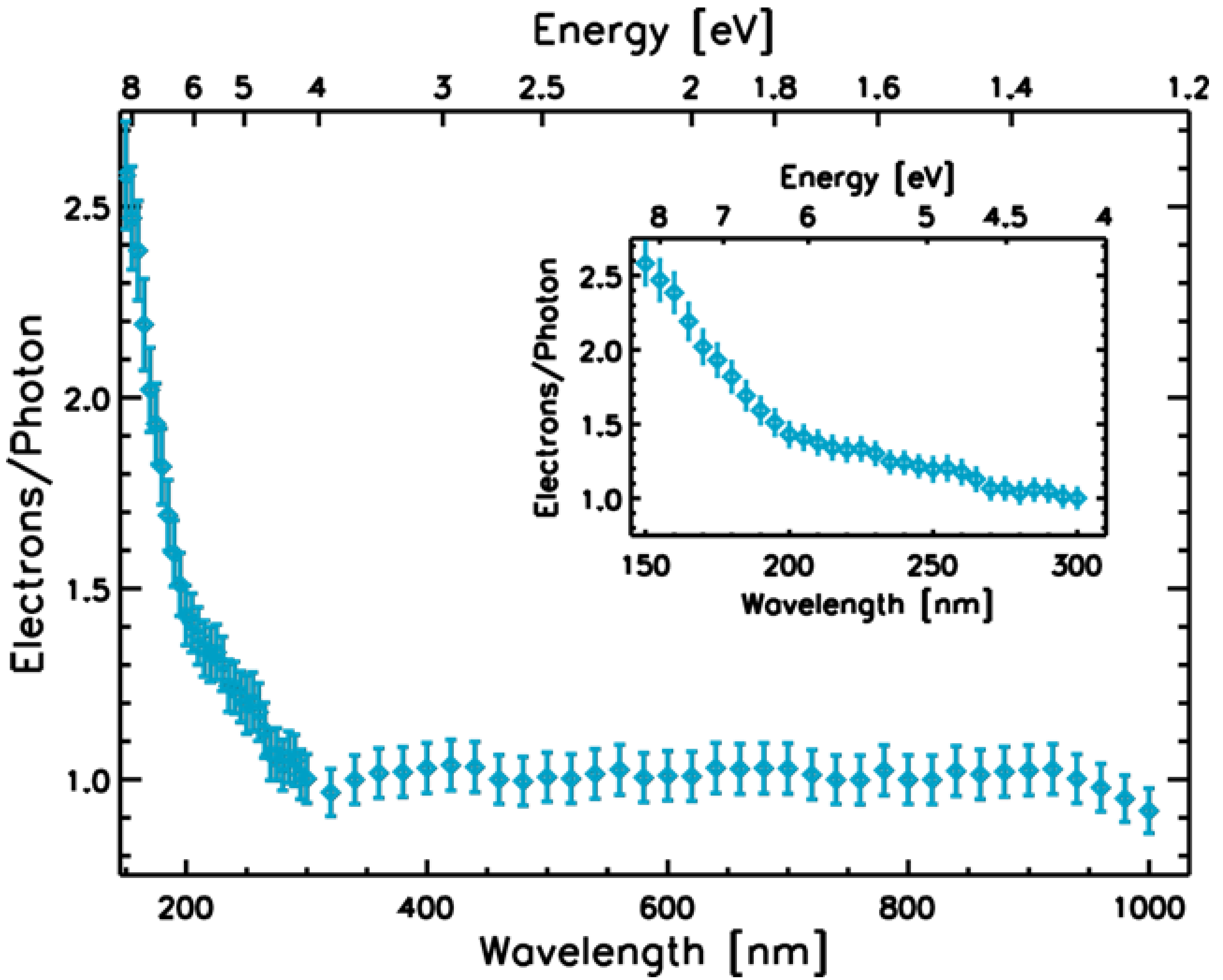

# Optical properties of the pnCCD

Measurement and calculations of optical response

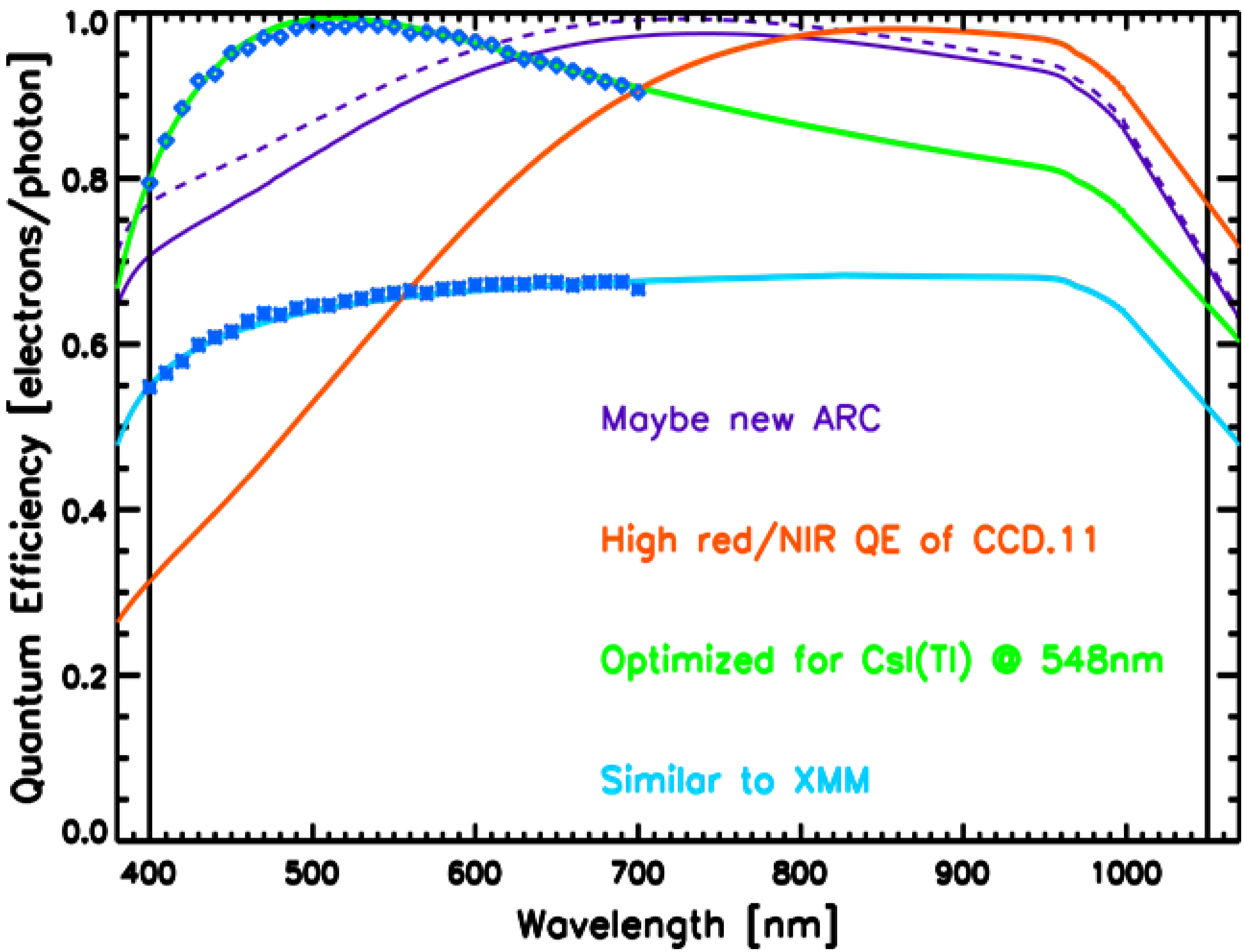

# Fast pnCCDs for single photon counting in the optical

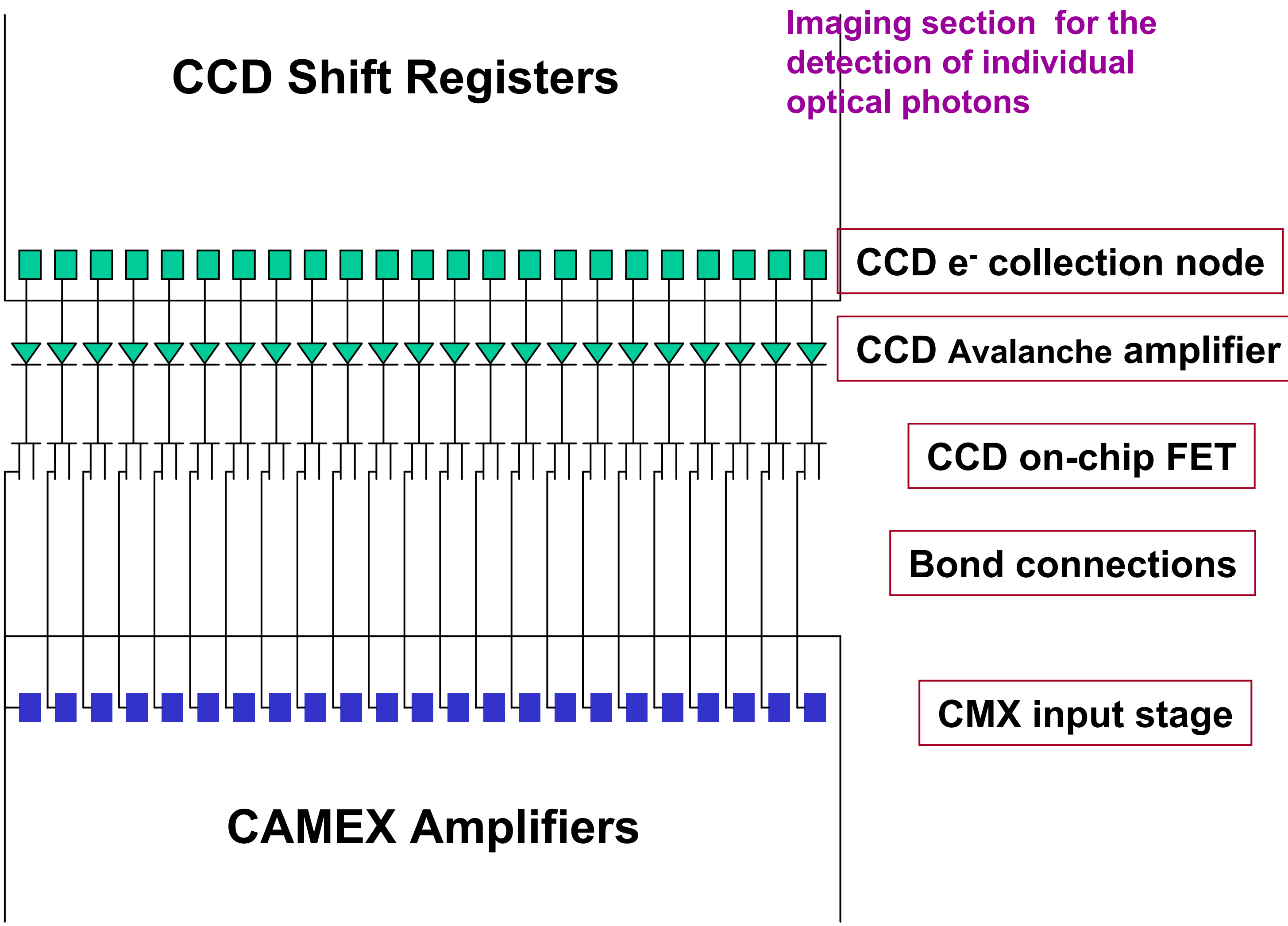

# The new concept

- **Basic idea:**
  - Move radiation entrance to backside of fully depleted device
  - Focus signal electrons on (small) avalanche region
- Development of concept to be shown in several steps

# Development of concept I

- Fully depleted bulk radiation entrance on backside
  - Adjustment of field needs large voltage variation

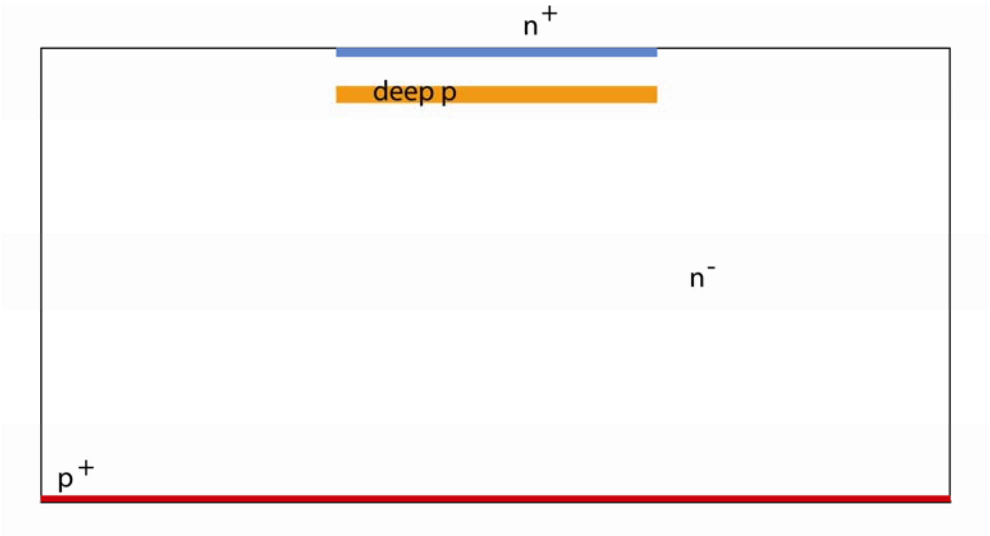

# Development of concept II

- Fully depleted bulk radiation entrance on backside
- Biasing from top ring-like structure
  - Gives better control of high field region

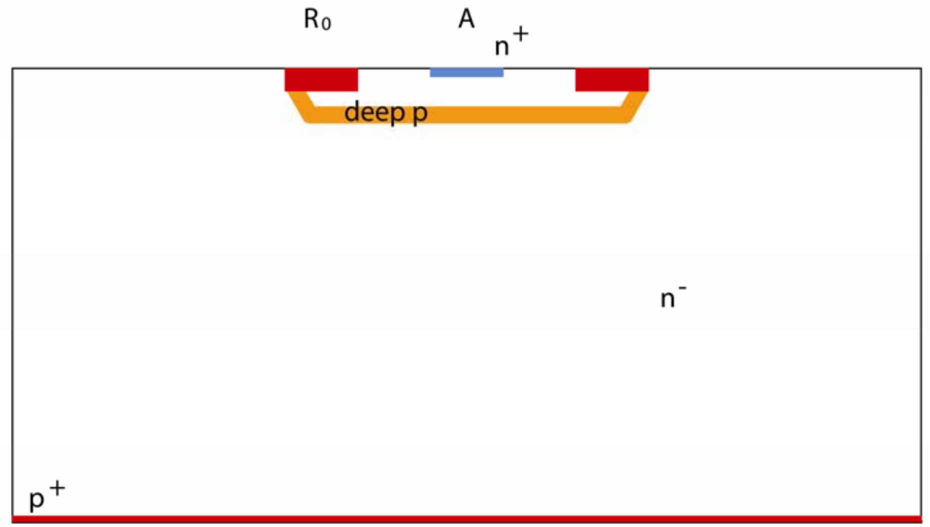

# Development of concept IV

- Fully depleted bulk radiation entrance on backside
- Biasing from top ring-like structure
  - Modulation of depth of buried p-layer
  - Addition of drift rings
  - Focusses electrons to centre

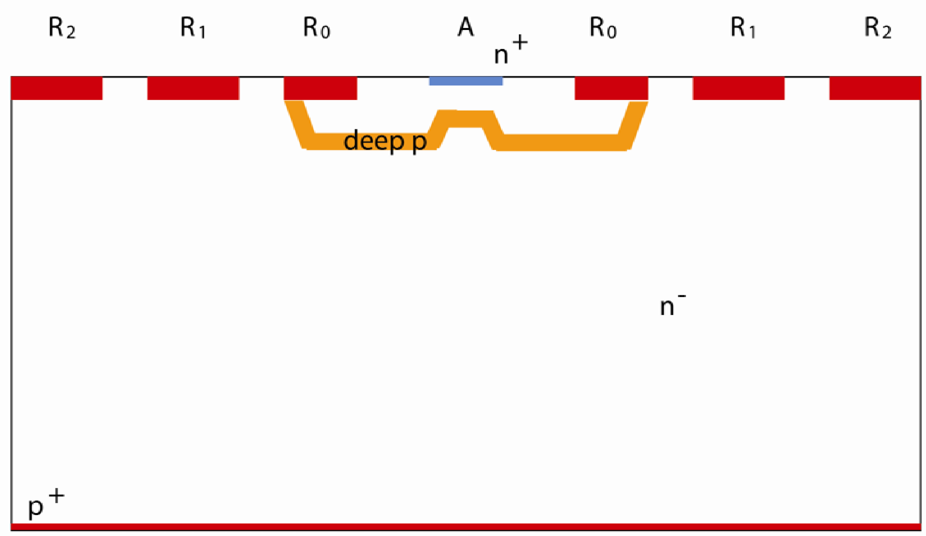

## Simulation results

- Electron and hole distribution around avalanche region

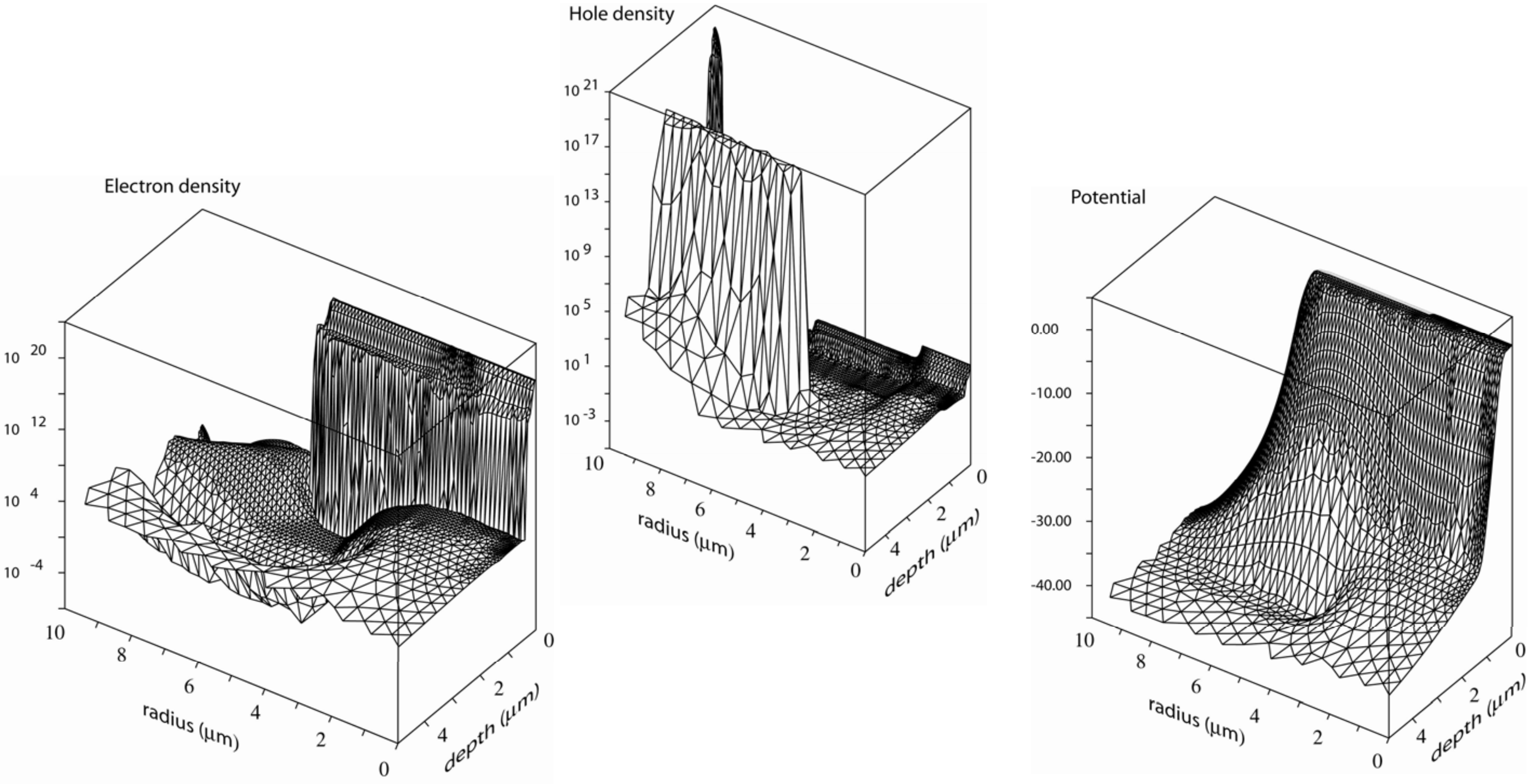

# Simulation results

- Electric field distribution in avalanche region
  - Uniform field distribution up to 3μm radius
  - All signal electrons enter avalanche region at smaller radius

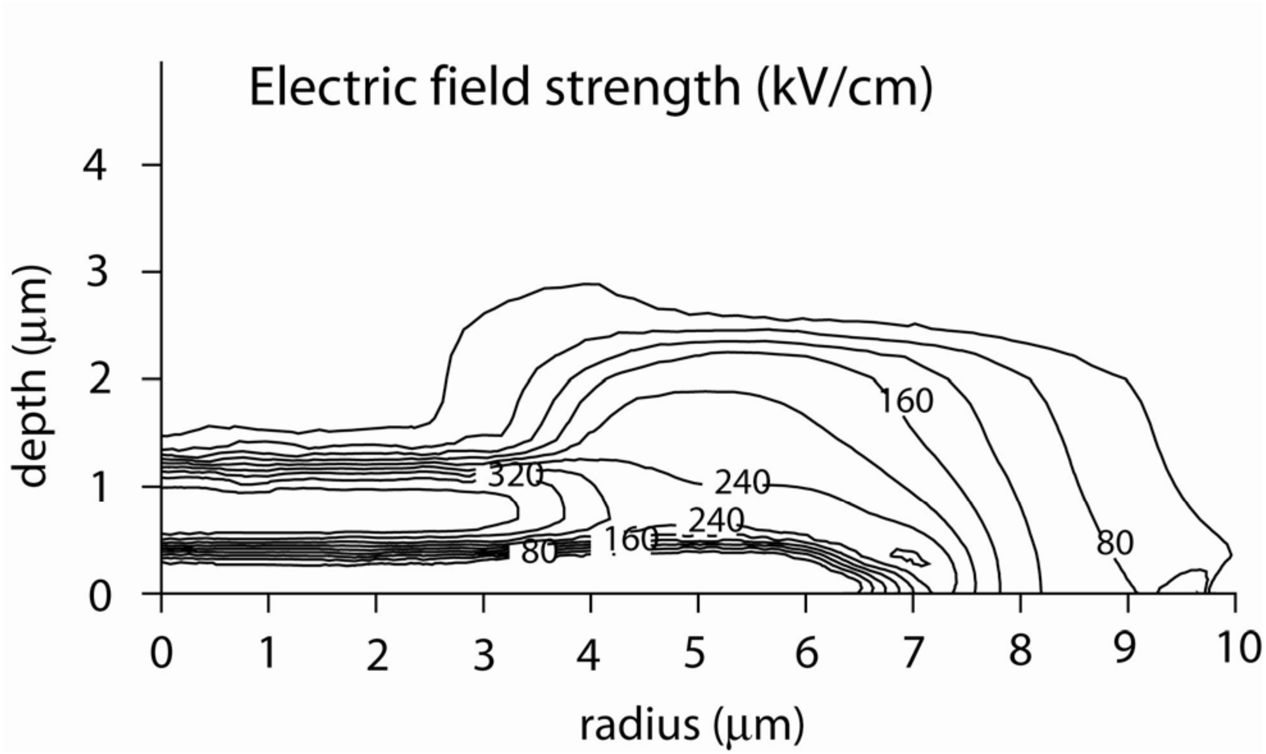

# Controlled-Drift Detector (CDD) - Working principle

(patents: EP 0862226, US 6,249,033)

## integration phase

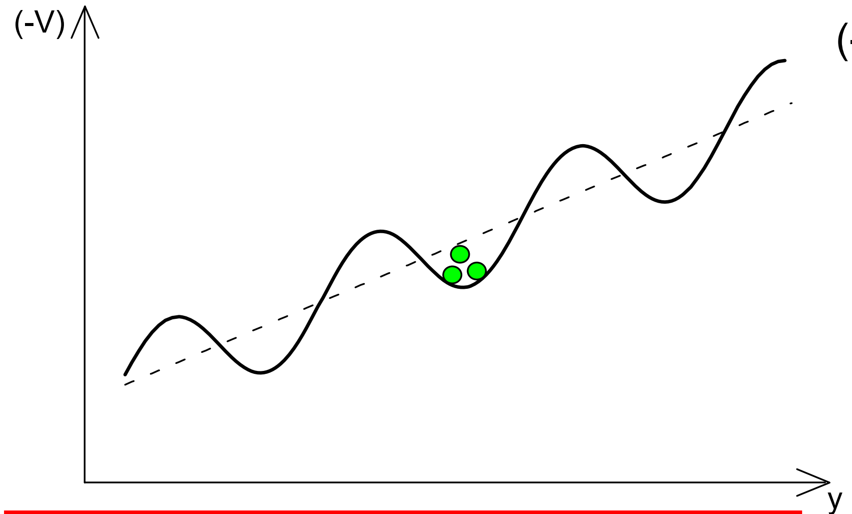


- **suitable perturbation** superposed to the linear bias **blocks the drift.**
- **integration wells** fully confine the signal electrons.

## drift phase

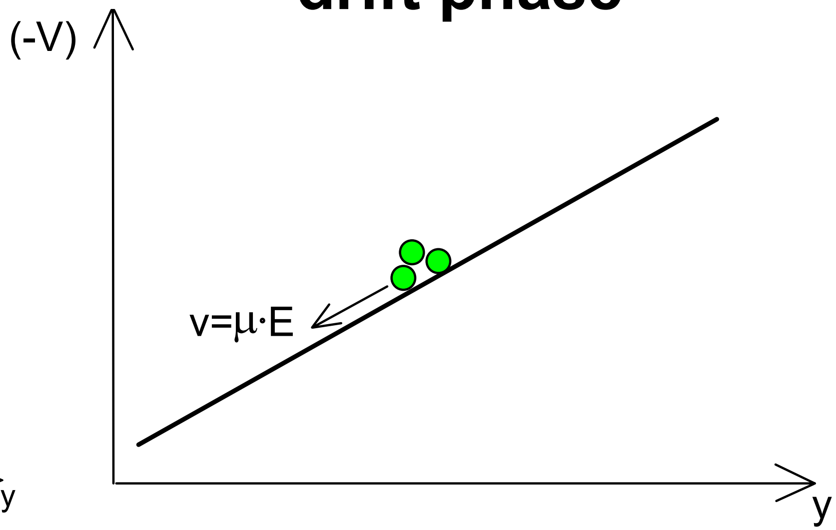


- the **barriers** that block the drift are **removed.**
- a **static field drifts** the signal electrons to the anodes.

# The Compton Camera Imager (CCI)

1. The Compton Camera Concept
2. The Controlled Drift Detector (CDD)
3. First Tests
4. Fast Timing

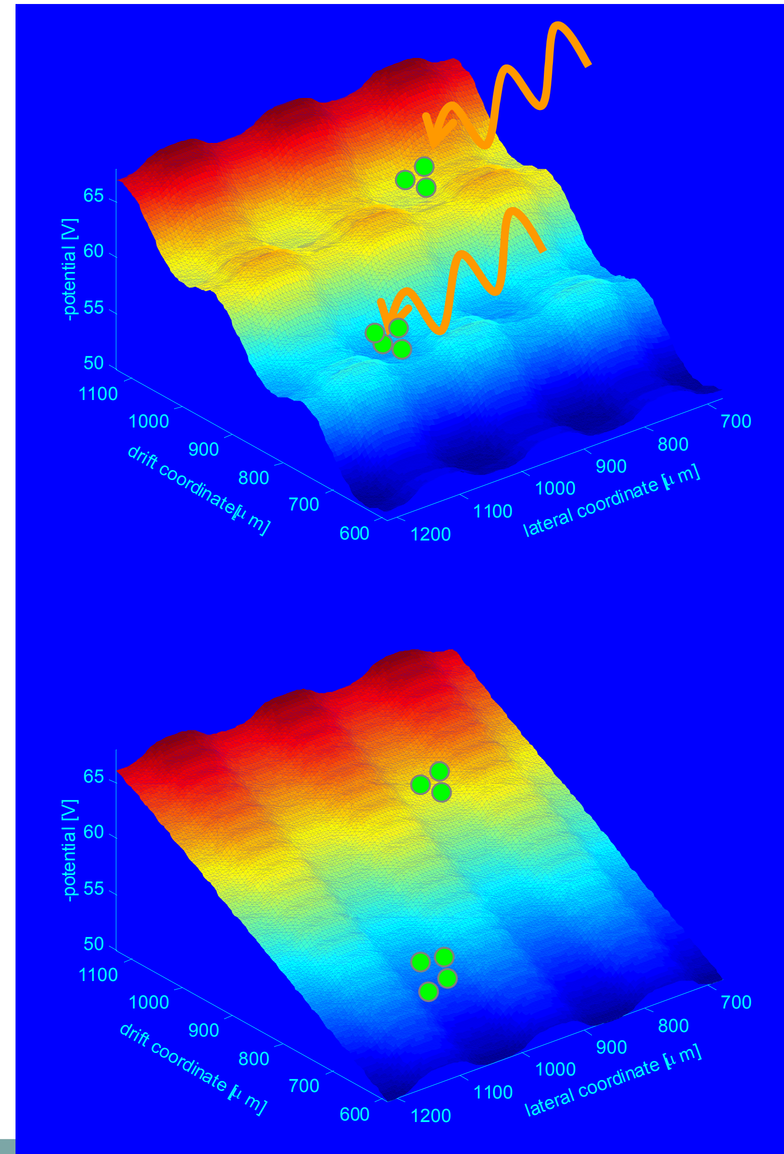


**Participating Institutions:**

1. Universität Siegen (D)
2. Politecnico di Milano (I)
3. MPE-HLL (D)
4. Universität Bonn (D)
5. Universität Essen (D)
6. Vanderbilt University (USA)
7. University College London (UK)
8. University of Rome (I)
9. Universität Erlangen (D)
10. Forschungszentrum Jülich (D)

# The basic concept of the Compton Camera

**Advantages of CCI´s for small animal analysis:**

1. Position resolution can be as good as 100 µm ($\Delta\delta \approx 0.5^o$)
2. CCI is operated colimatorless
3. Total efficiency can be as high as 10 %
4. Performance gain with increasing X-ray energy
5. No inverse relation between resolution and sensitivity
6. Good intensity resolution

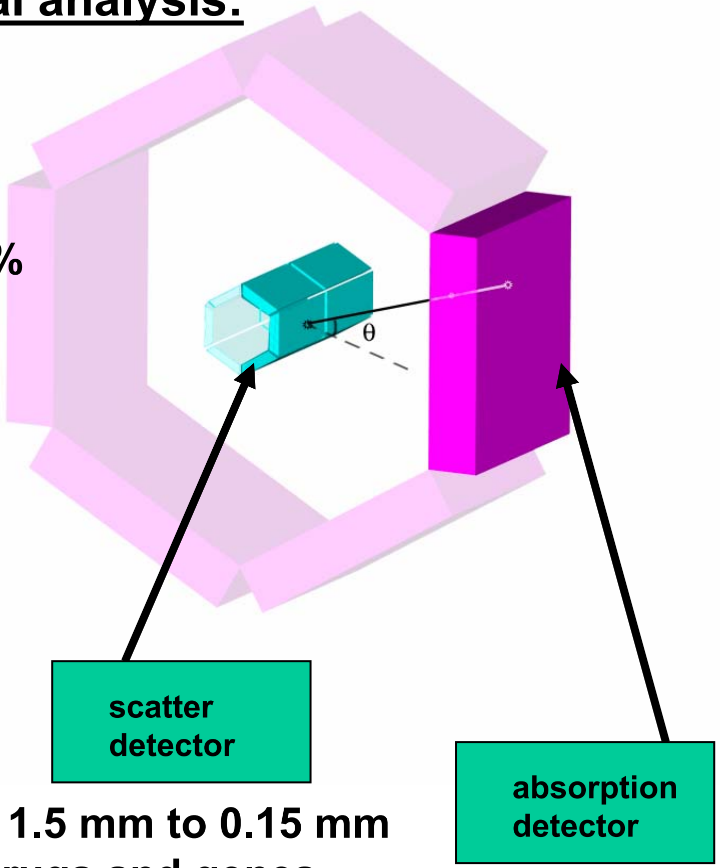


**Our goals:**

1. Improve in vivo image resolution from 1.5 mm to 0.15 mm
2. Determine the distribution of labeled drugs and genes with increased accuracy
3. Verify the targeting of receptor specific probes for clinical utility and drug development
4. ....

# The Compton Camera Imaging Concept

$$\cos\theta = 1 - \frac{m_e\, c^2}{E_{\gamma'}} + \frac{m_e\, c^2}{E_{\gamma'} + E_e}$$

$$\Delta\theta_E = \frac{\left[1 + \frac{E_\gamma}{m_e c^2}(1-\cos\theta)\right]^2}{\frac{E_\gamma^2}{m_e c^2}\sin\theta}\Delta E_e$$

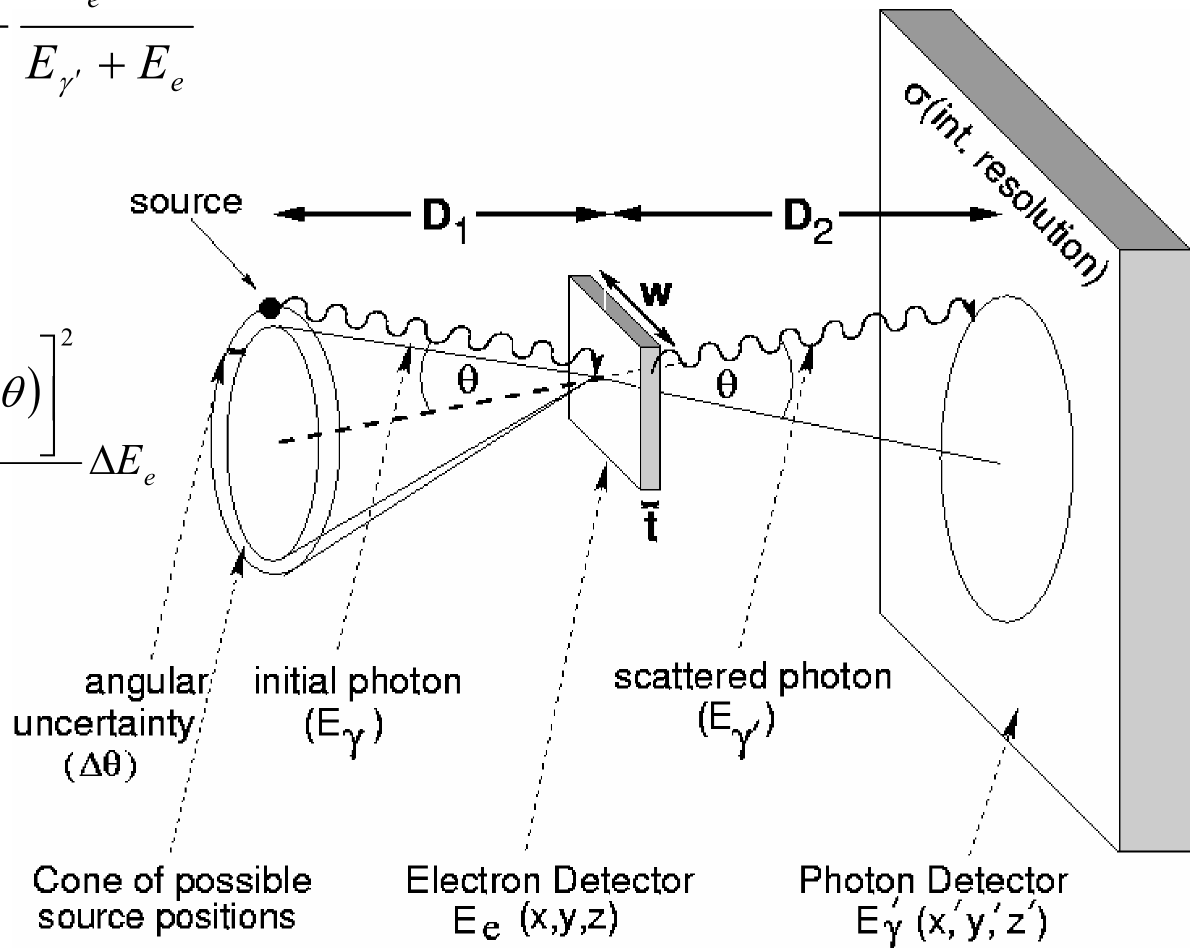

# SDDs with fast trigger for event coincidence in drift detectors: The Controlled drift detector

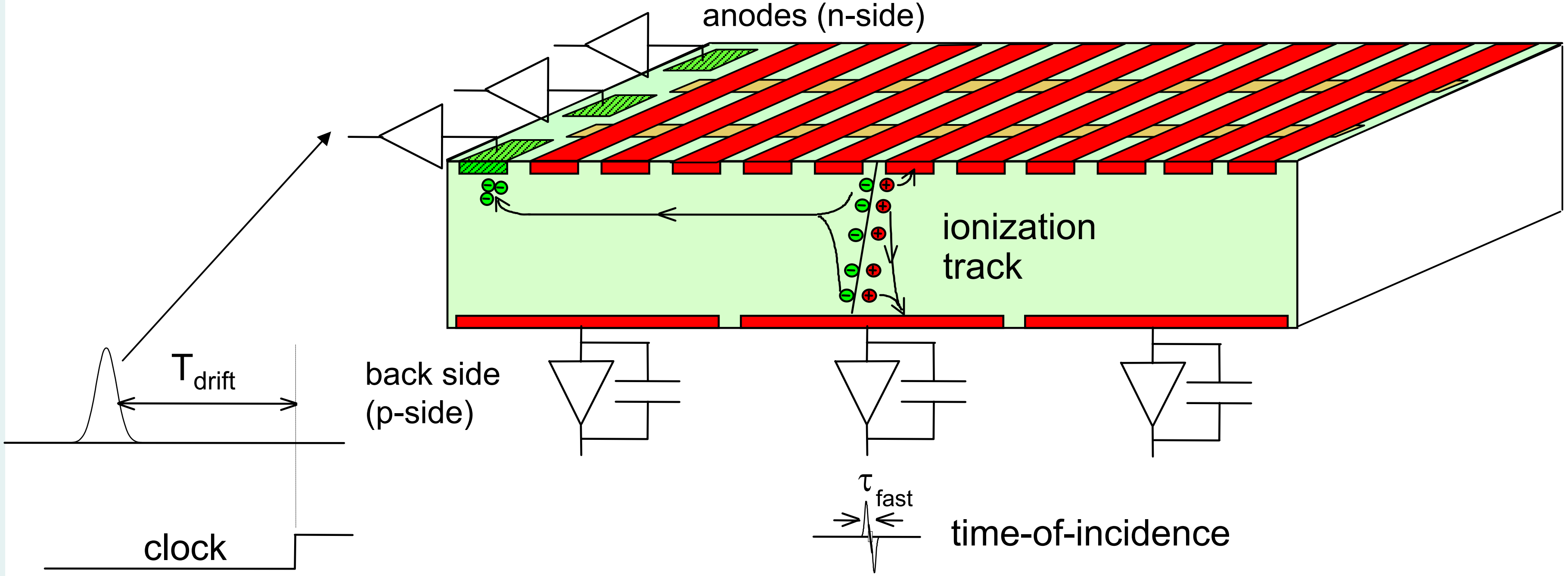


- fast trigger from electron-hole induction on back electrodes
- achievable time jitter depends on induction signals, electronic noise, etc..

# 2-D imaging and spectroscopy of a Fe-55 source @ 100 kHz

A.Castoldi, C.Guazzoni, P.Rehak, L.Strüder, Trans. Nucl. Sci. 49 (3) June 2002

Δt = 55 ns

FWHM = 11 ns

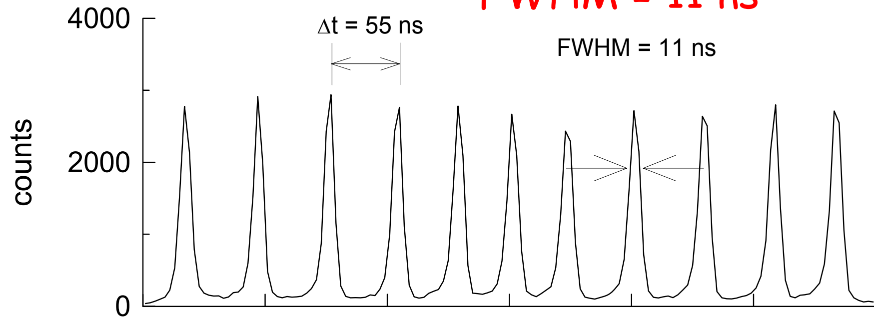


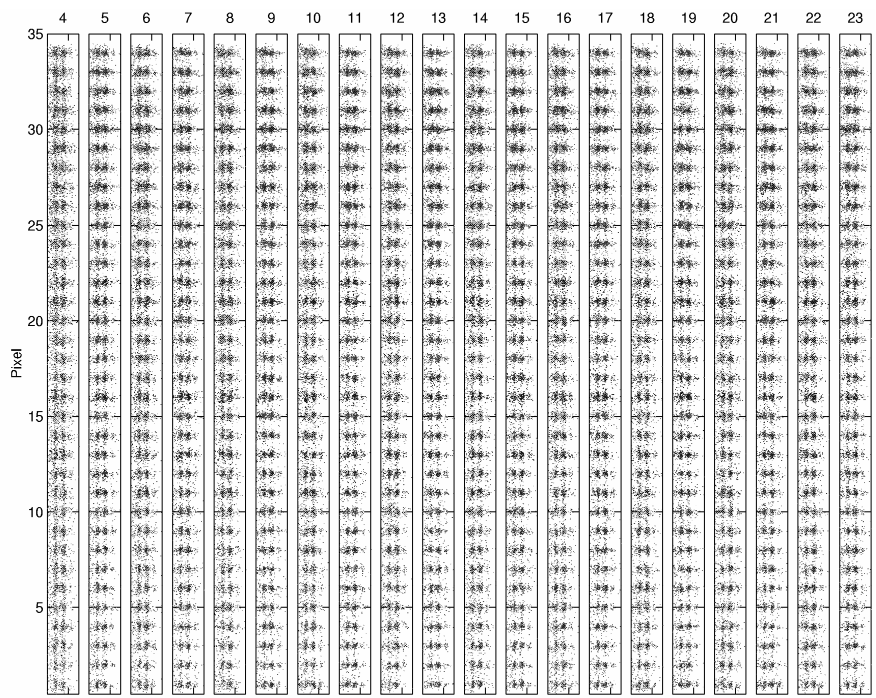


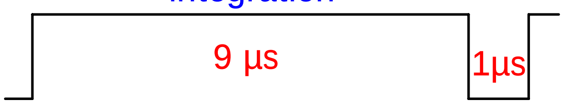


Frame frequency=100 kHz

Pixel 180μm x 180μm

~250 eV FWHM @ 300K
(ENC=26 eletrons r.m.s.)

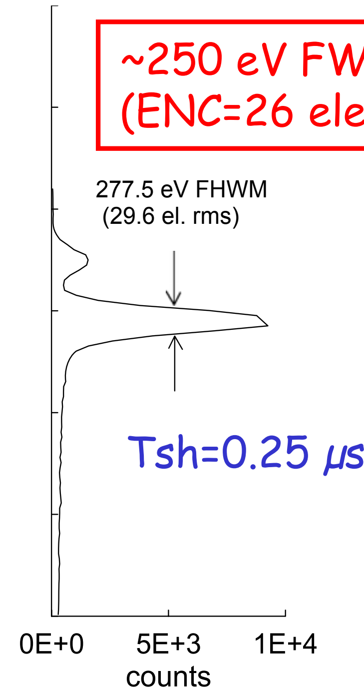


**Photograph of 6x6 mm² CDD prototype**

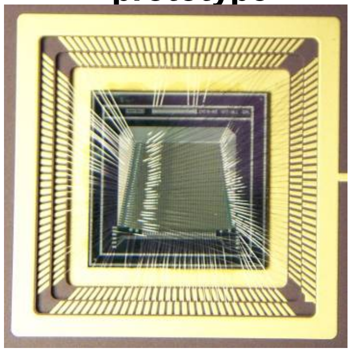

# X-ray spectroscopy/imaging tests with CDDs

*Radiographic image of a lizard*...*

*pixel size: 120$\mu$m, $10^5$ frames/s, T=300 K*

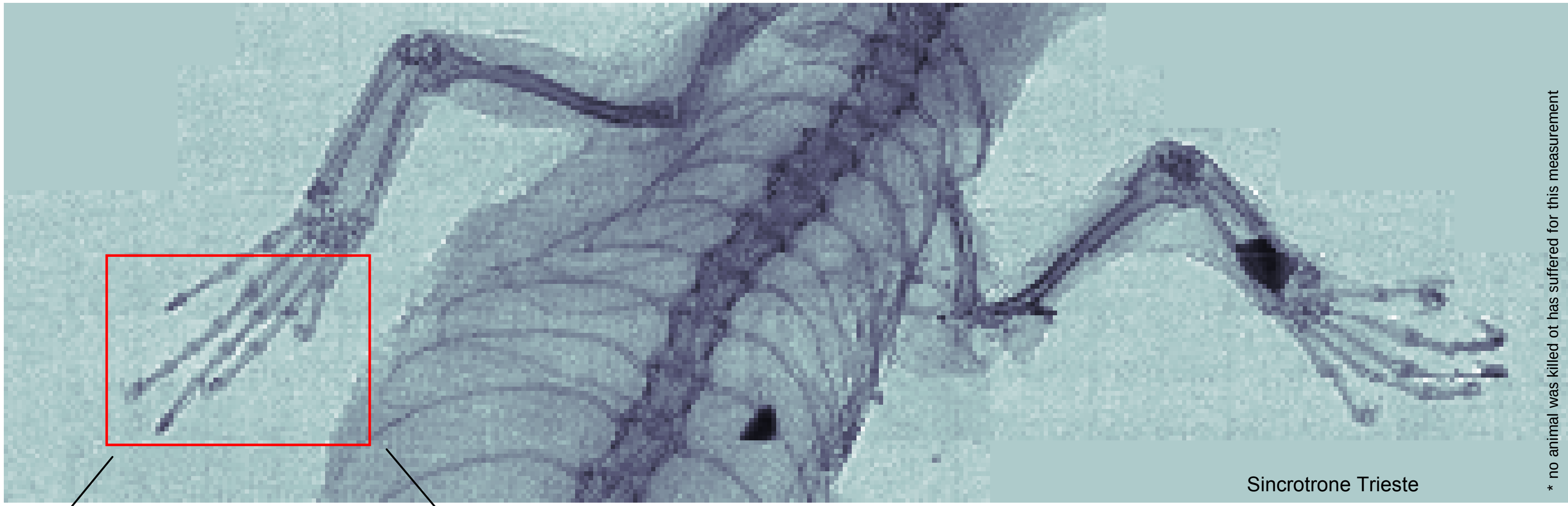


* no animal was killed ot has suffered for this measurement

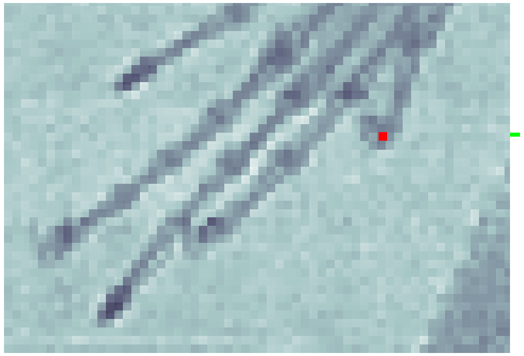

*...and spectroscopic analysis of each pixel*

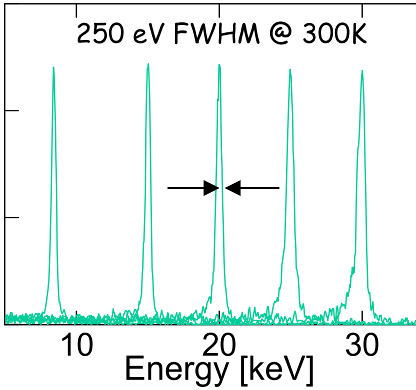

# First experimental results

Pulsed IR 904 nm laser (pulse duration <100ps)

## Output waveform

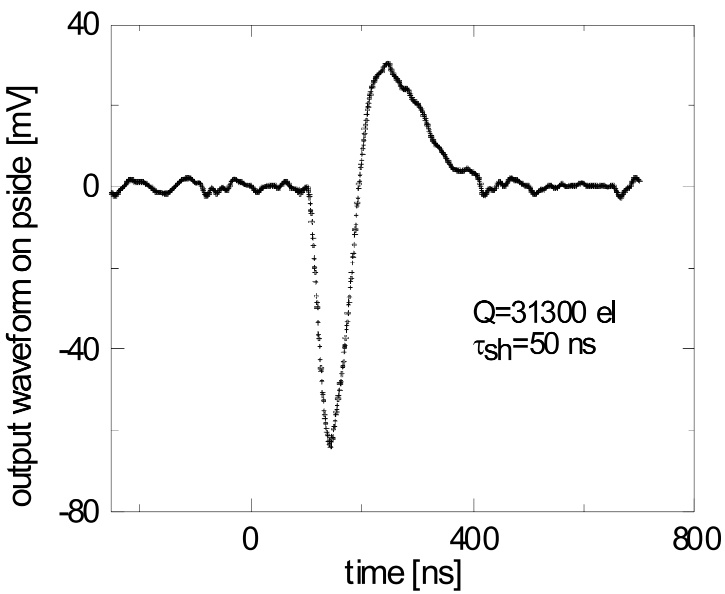


## Measured time jitter @ Q=31300 el

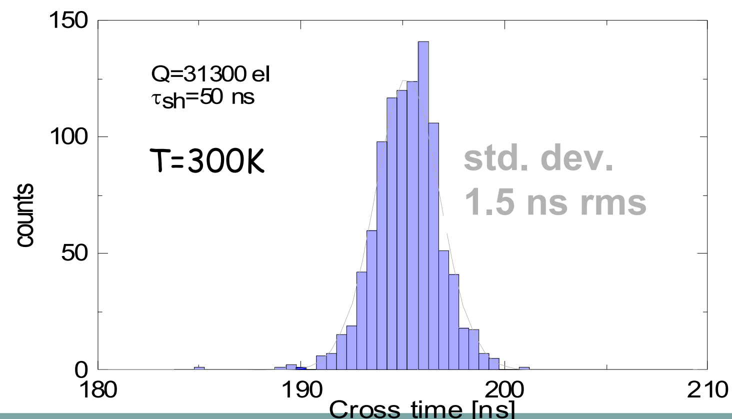


## Time jitter vs. signal charge Q

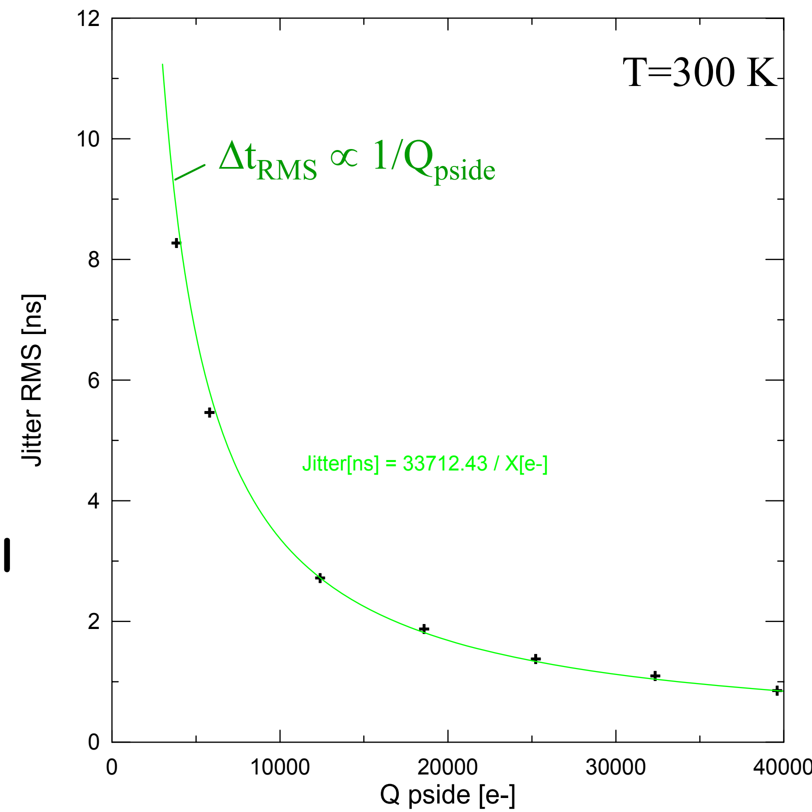

# The DEPMOSFET active pixel sensor

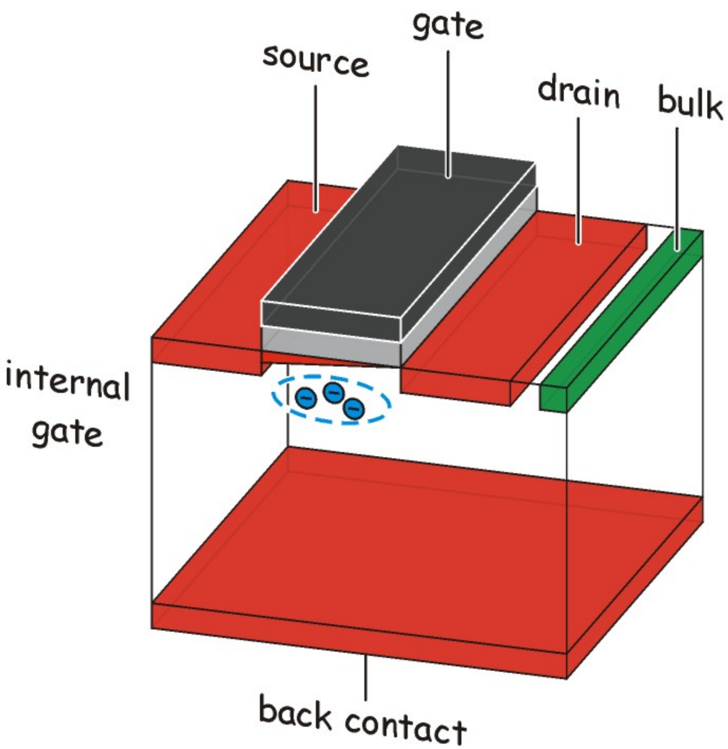


**1 electron increase current by 0.3 nA to 1 nA**

**electrons stored in the internal gate increase source-drain current**

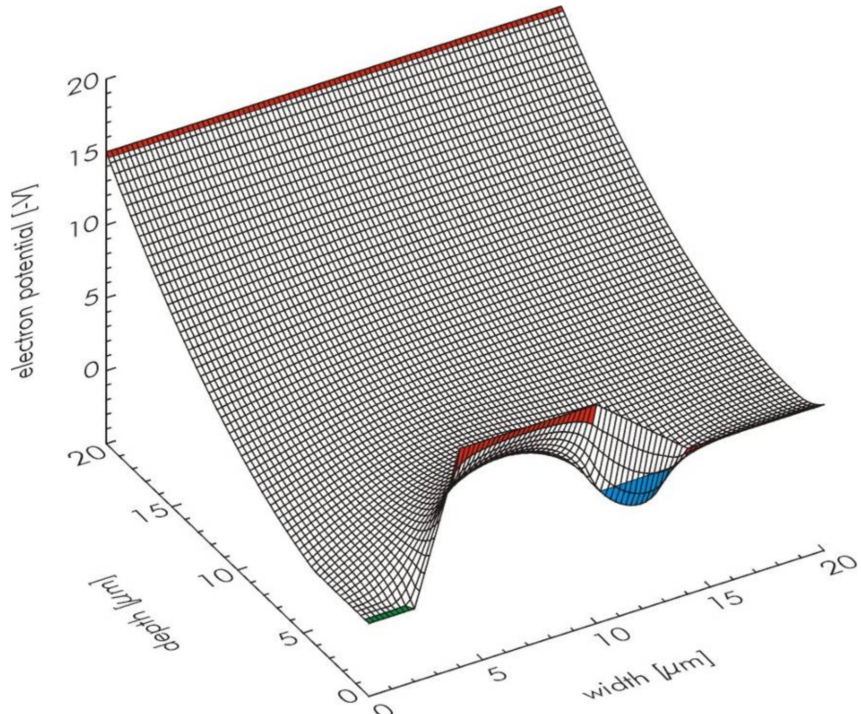

# The DEPMOSFET for XEUS and ILC

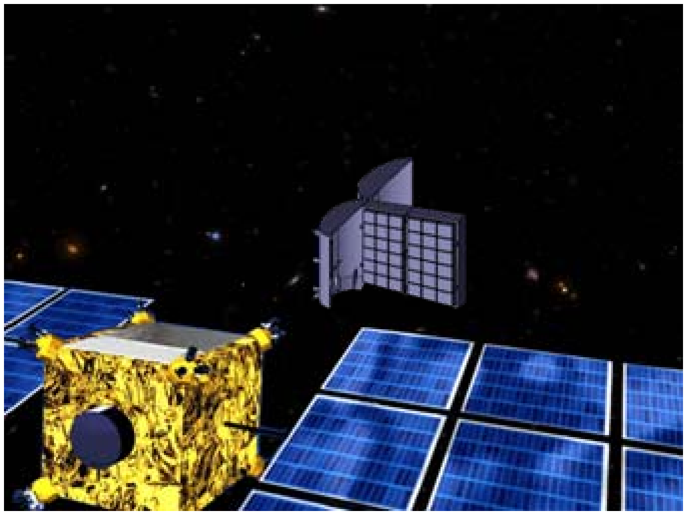

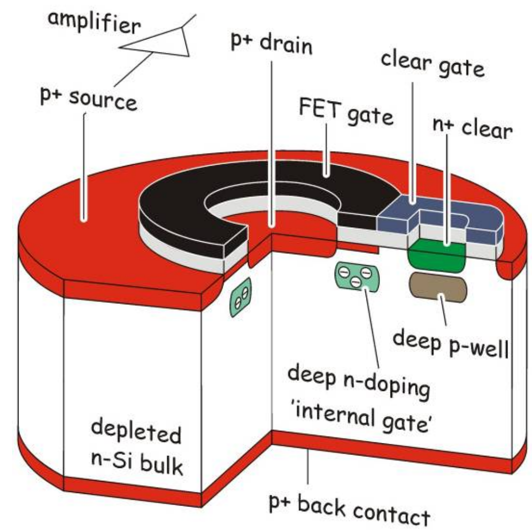


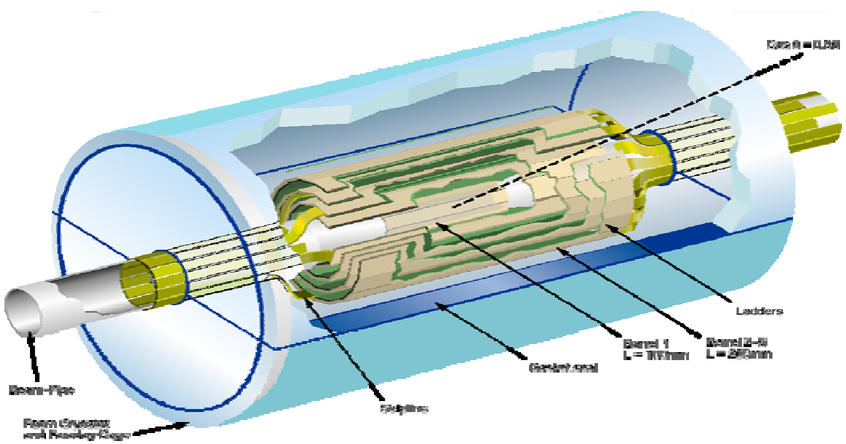


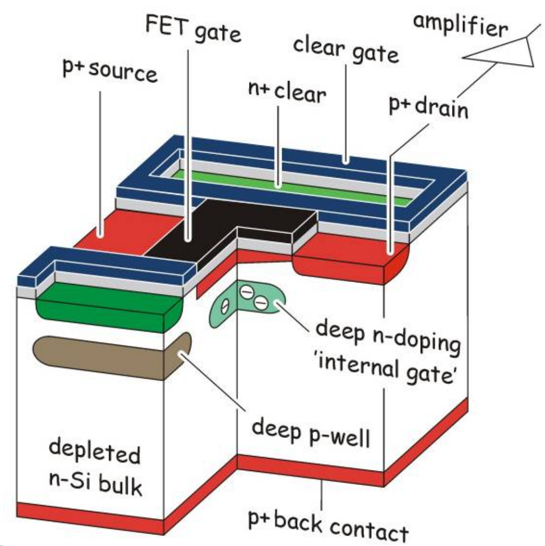

# The future in X – rays: The XEUS mission

ASCA´s and
XMM´s relativistic
Fe-line
Tanaka et al. 1995

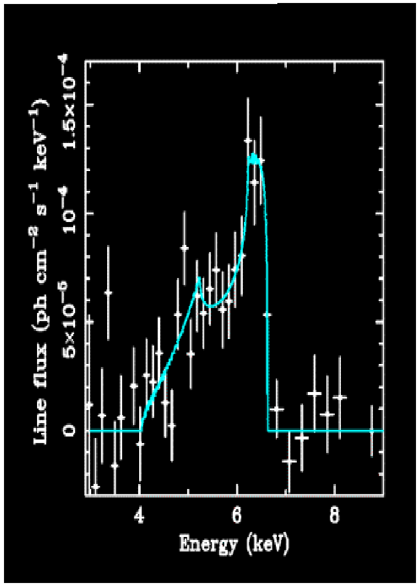


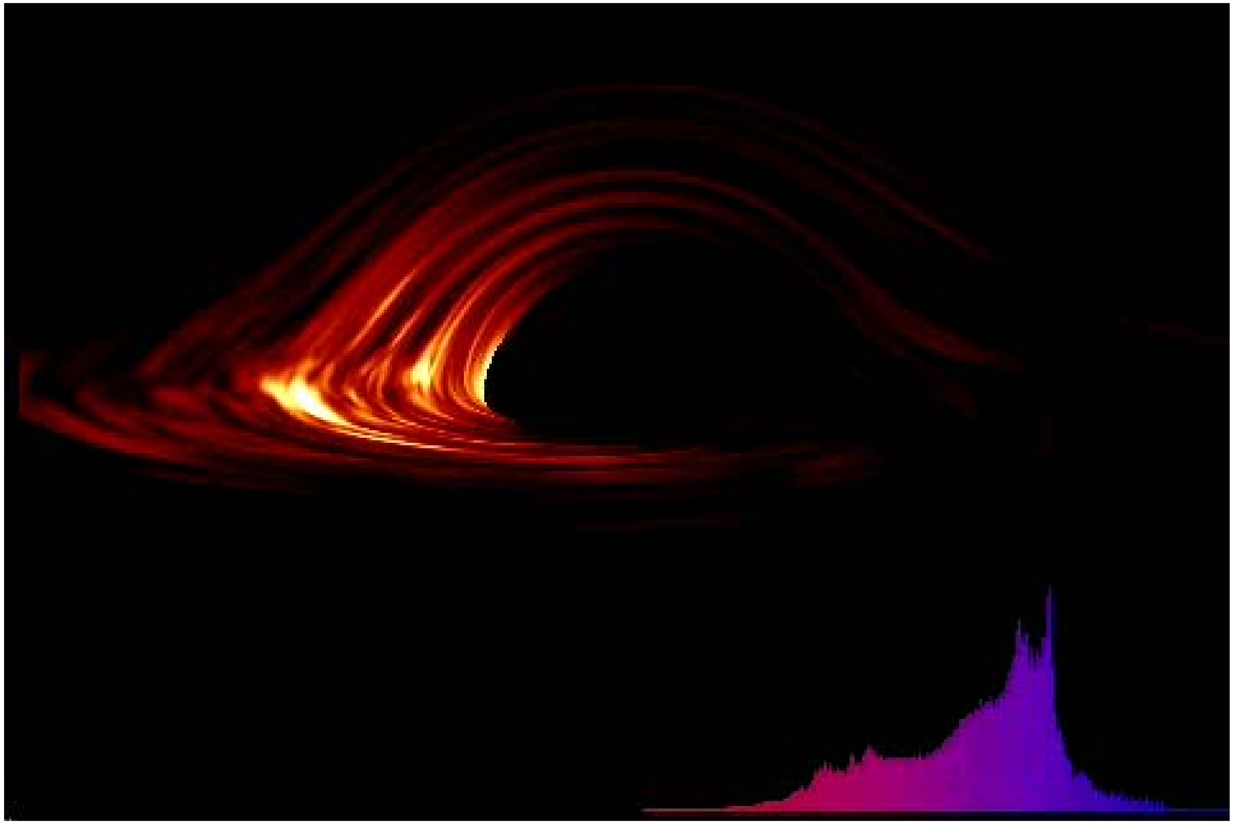

courtesy of Chris Reynolds

# DEPFETs for the XEUS WFI

1. Flexible operating modes
2. small power dissipation
   (less than 2 W)
3. Fano limited energy resolution
   from 0.3 keV to 30 keV
4. Spatial resolution better than
   15 µm @ 100 µm pixel size
5. Homogeneous radiation
   entrance window
6. Intrinsic radiation hardness,
   no charge transfer needed
7. ENC can be lowered to less
   than 1 $e^-$ rms with NDR
8. Optical ``Blocking Filter´´
   can be directly integrated
9. Operation at ``warm temperatures´´, e.g. – 40 ° C

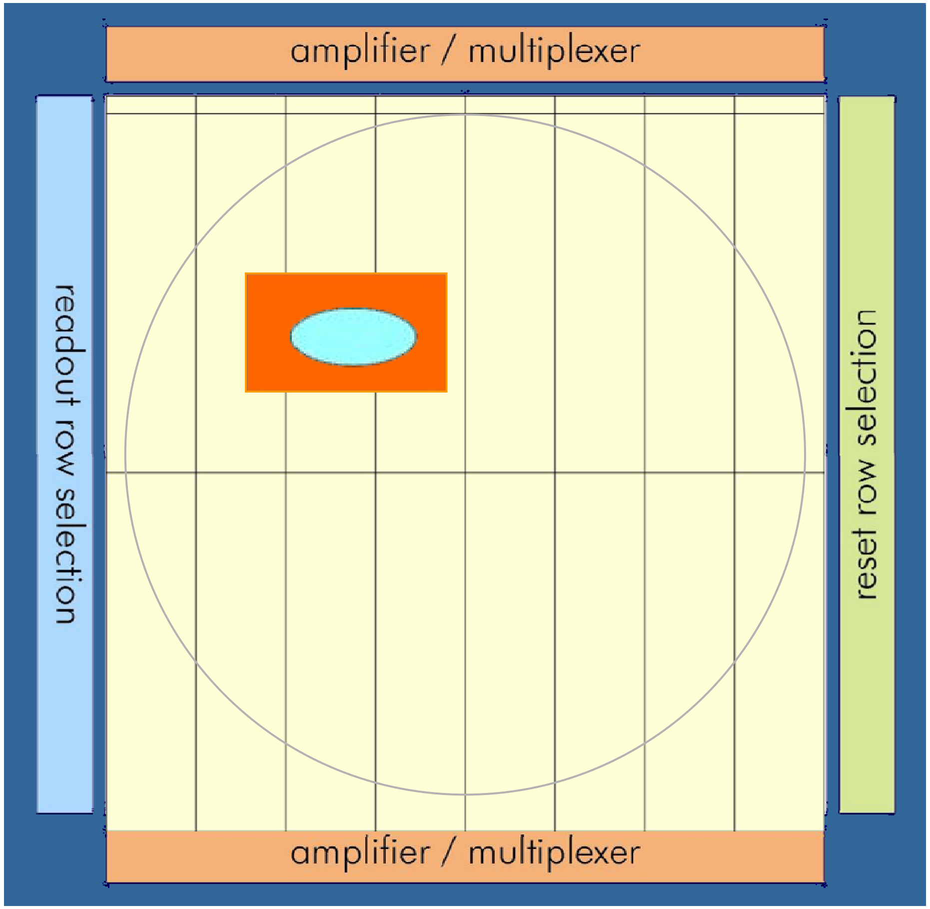

# Circular DEPMOSFET pixels

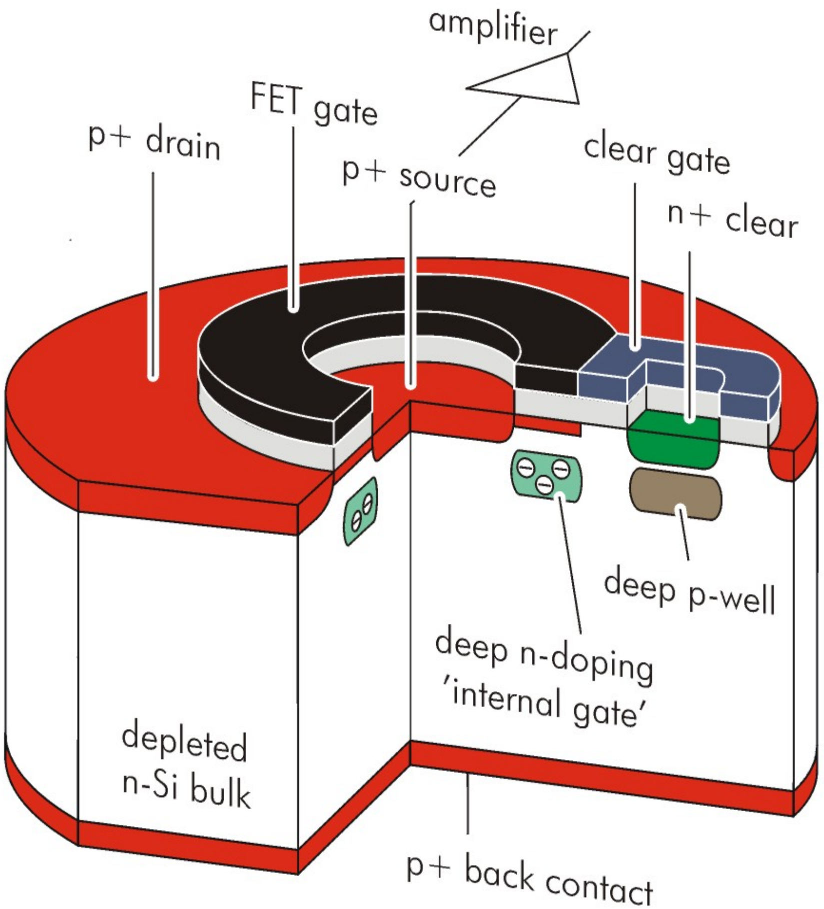


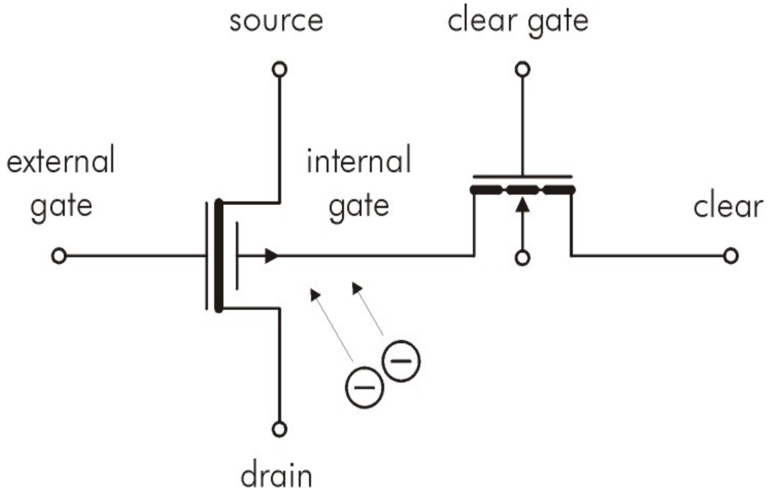

# DEPMOSFET matrix prototypes

- Global drain contact
- Sources connected column-wise
- Gate, Clear & Cleargate connected row-wise
- Source follower readout: Column biased by current source

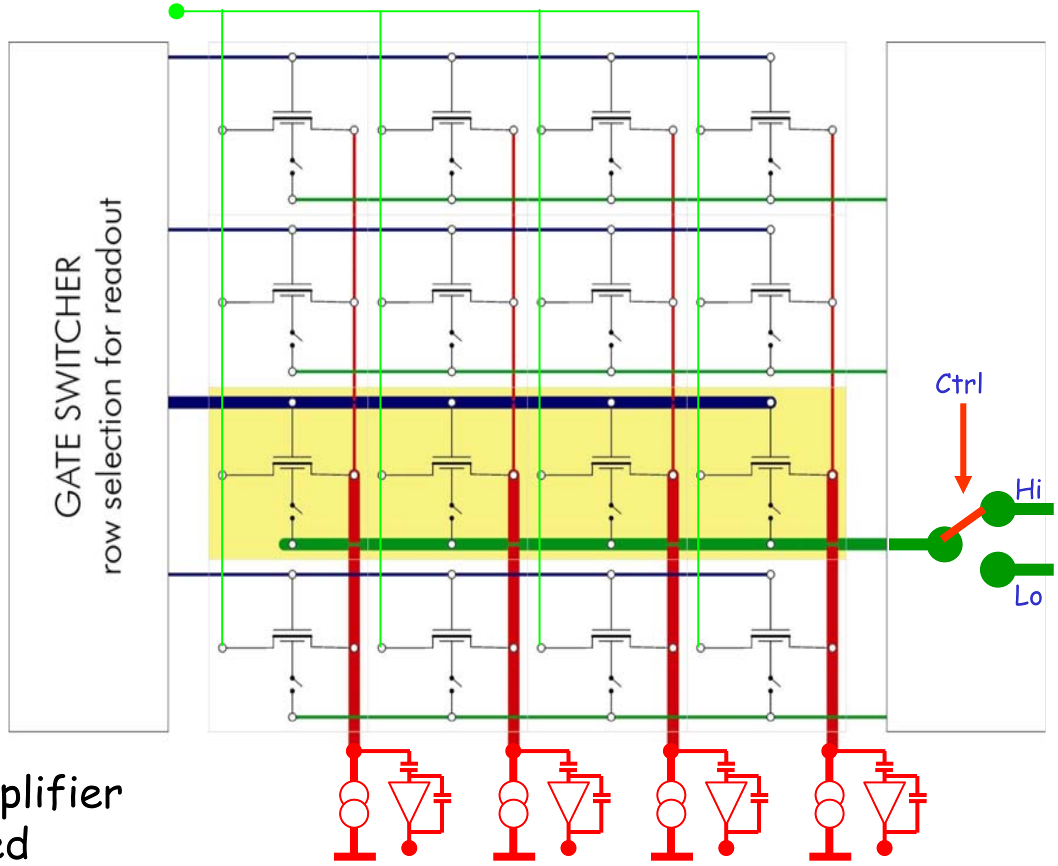


**CAMEX 64 G:**
64 channel low noise voltage amplifier
8-fold CDS-filter and integrated sequencer

**Switcher II:**
Control chip with 64 channels a 2 ports & integrated sequencer
AMS high voltage CMOS process (up to 20 V)

# Most favourable design

- **STD: 45 μm gate circumference / 5 μm Gate length**

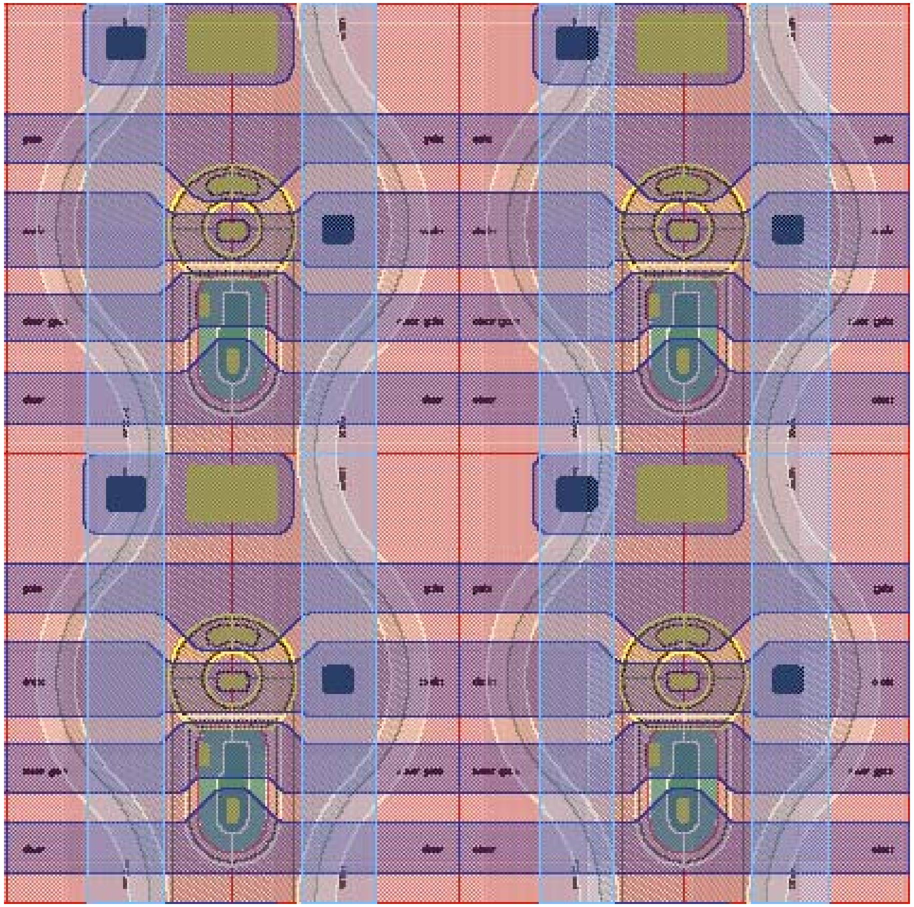

**All structures with 2 polysilicon and 2 metal layers**

**Structures of this type homogeneous and defect free**

# Prototype matrices

- 64 x 64 pixel arrays with 75 x 75 $\mu m^2$ pixel size
- Complete set of control & readout electronics
- 2 kinds of hybrids: PCB & Ceramic
- PCB for pre-testing and structure selection
- Ceramic for high-performance tests at low temperature
- Modular, PC based and scalable readout system for test & evaluation

- PCB type Hybrid

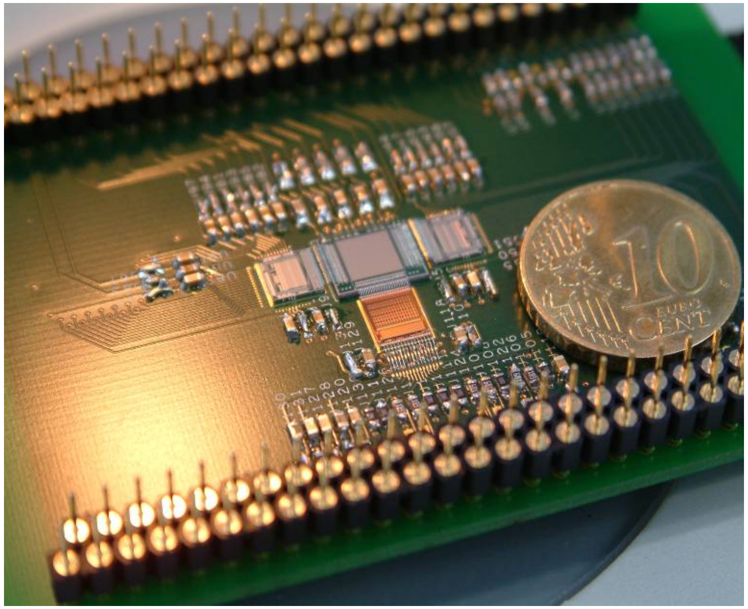

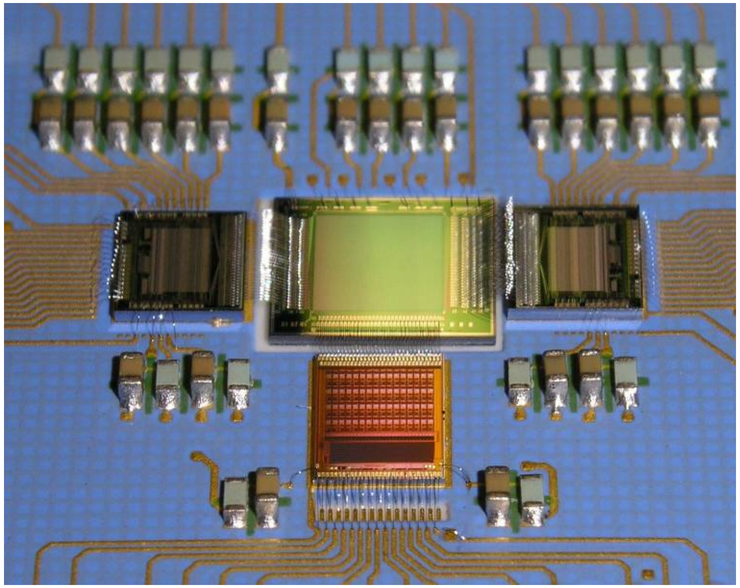

- Ceramic Hybrid

# Energy resolution of DEPMOSFET arrays

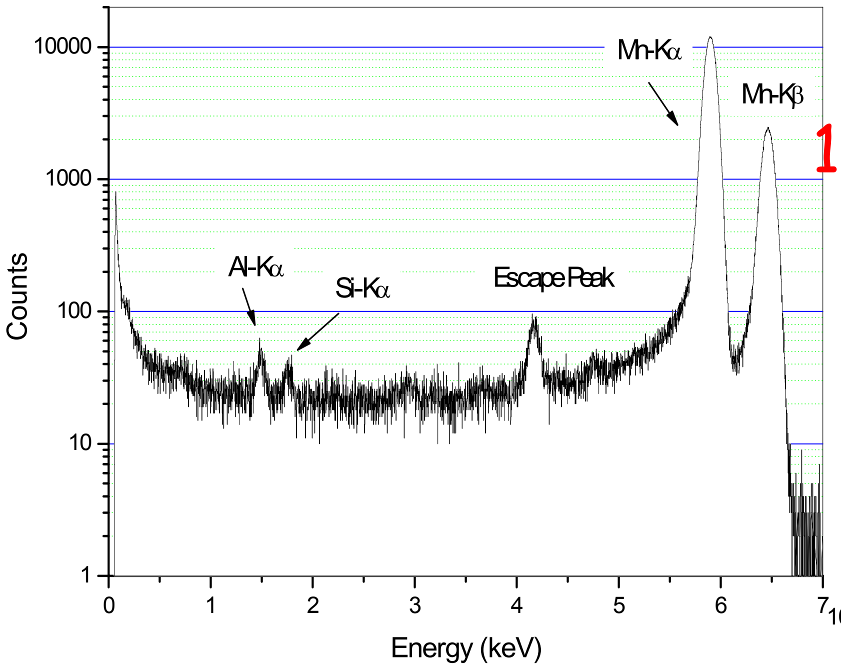


"Frontside" illumination:
Source illuminates electronic side

Energy resolution:
131 eV FWHM @ Mn-Ka Line
corresponding to 6.4 $e^-$ ENC

Energy resolution:
133 eV FWHM @ Mn-Ka Line
corresponding to 6.9 $e^-$ ENC

"Backside" illumination:
Source on top of entrance window

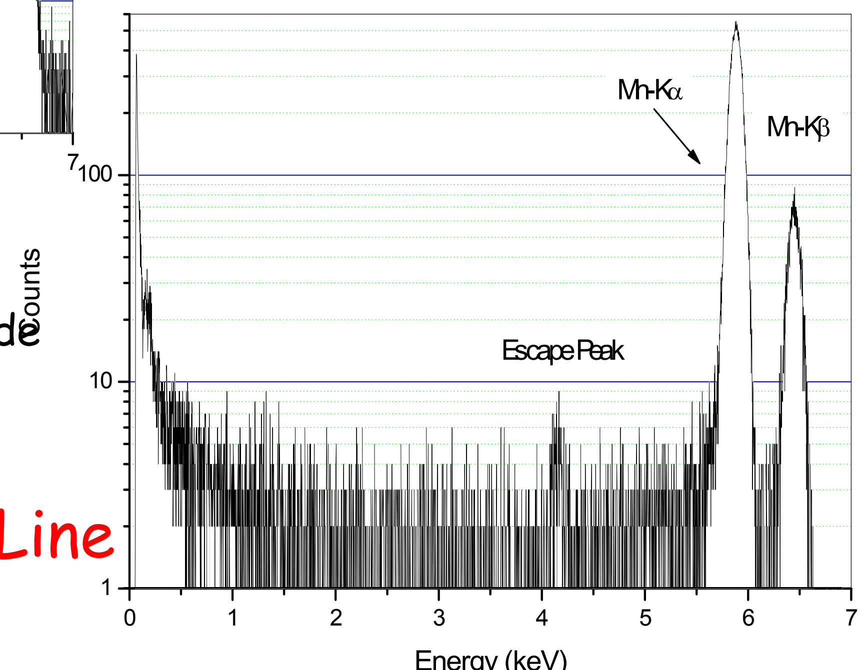

# Imaging with DEPFETs

- Illumination from backside
- Baffle: 300 μm thick silicon
- Minimal structure size: 150 μm
- Exposure ca. 100000 frames

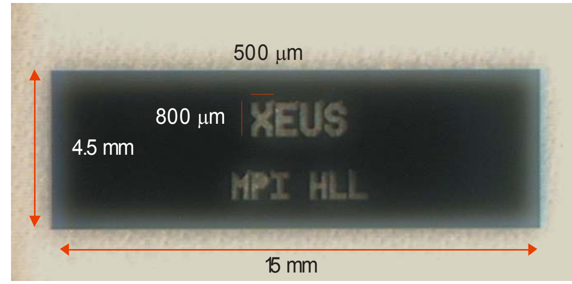


- Contour plot from ADU maps

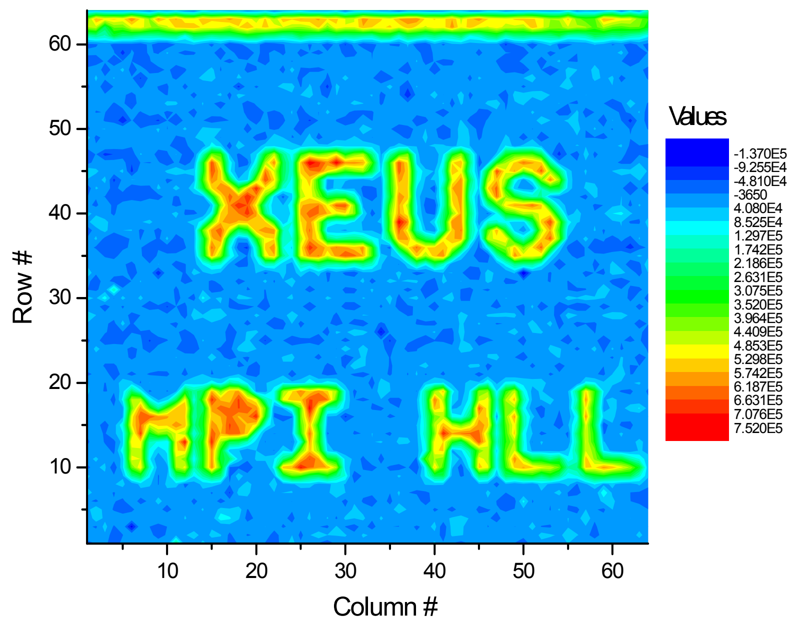


- Hitmap with 100 ADU threshold

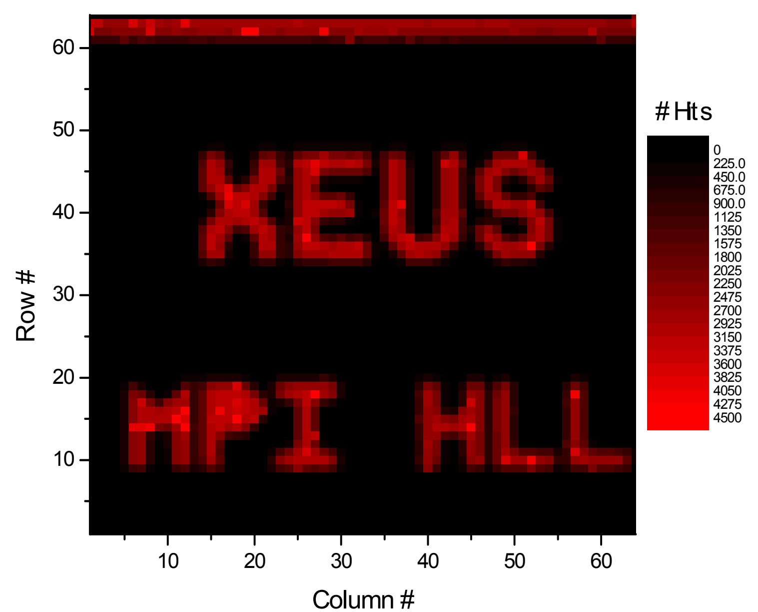

# Scientific activities of the MPE